

Review

Recent Developments in Tandem White Organic Light-Emitting Diodes

Peng Xiao ¹, Junhua Huang ¹, Yicong Yu ^{1,*} and Baiquan Liu ^{2,3,*}

¹ School of Physics and Optoelectronic Engineering, Foshan University, Foshan 528000, China; xiaopeng@fosu.edu.cn (P.X.); jamha1212@163.com (J.H.)

² LUMINOUS! Centre of Excellent for Semiconductor Lighting and Displays, School of Electrical and Electronic Engineering, Nanyang Technological University, Nanyang Avenue, Singapore 639798, Singapore

³ Institute of Polymer Optoelectronic Materials and Devices, State Key Laboratory of Luminescent Materials and Devices, South China University of Technology, Guangzhou 510640, China

* Correspondence: yicong2007@gmail.com (Y.Y.); l.baiquan@mail.scut.edu.cn (B.L.)

Received: 7 December 2018; Accepted: 25 December 2018; Published: 2 January 2019



Abstract: Tandem white organic light-emitting diodes (WOLEDs) are promising for the lighting and displays field since their current efficiency, external quantum efficiency and lifetime can be strikingly enhanced compared with single-unit devices. In this invited review, we have firstly described fundamental concepts of tandem device architectures and their use in WOLEDs. Then, we have summarized the state-of-the-art strategies to achieve high-performance tandem WOLEDs in recent years. Specifically, we have highlighted the developments in the four types of tandem WOLEDs (i.e., tandem fluorescent WOLEDs, tandem phosphorescent WOLEDs, tandem thermally activated delayed fluorescent WOLEDs, and tandem hybrid WOLEDs). Furthermore, we have introduced doping-free tandem WOLEDs. In the end, we have given an outlook for the future development of tandem WOLEDs.

Keywords: tandem; organic light-emitting diode; white; charge generation layer; doping-free

1. Introduction

In recent years, organic light-emitting diodes (OLEDs) have entered the mainstream display market, since they can show comparable performance with the liquid crystal displays [1–5]. Besides, OLEDs are promising for the solid-state lighting, which may be able to compete with GaN-based LEDs [6–10]. This is because OLEDs possess many merits, including high efficiency, low power consumption, broad viewing angle, fast response, thin thickness, solution-processed compatibility as well as flexibility [11–16]. With the evolution of emitters and enhancement of device engineering, both phosphorescent and thermally activated delayed fluorescence (TADF) materials-based OLEDs can realize a theoretical unity internal quantum efficiency (IQE) due to the harvest of totally singlet and triplet excitons [17–20]. For phosphorescent materials, they harness singlets and triplets due to the heavy-atom effect [21–23]. In terms of TADF emitters, a small energy gap for triplet excited state (T_1) and singlet excited state (S_1) is required, which is beneficial to the reverse intersystem process for the 100% exciton harvesting efficiency [24–26].

To further promote the OLED technology for high-quality displays and energy-saving lighting field, white OLEDs (WOLEDs) have vastly attracted both industrial and academic interest [27–31]. In 1994, the first WOLED was developed by Kido and coworkers, showing a maximum power efficiency (PE) of 0.83 lm W^{-1} [32,33]. Over the last twenty-four years, the performance of WOLEDs has been remarkably enhanced. By dint of phosphorescent emitters and advanced outcoupling technique, the PE of WOLEDs could show a PE of 123.4 lm W^{-1} at the illumination-related luminance of 1000 cd m^{-2} with

an external quantum efficiency (EQE) of 54.6%, which remains 106.5 lm W^{-1} at an ultrahigh luminance of 5000 cd m^{-2} [34]. Even for flexible phosphorescent WOLEDs, their PE can overtake 100 lm W^{-1} [35]. Currently, the EQE of TADF emitter-based WOLEDs has also been demonstrated to exceed 20% [36–39]. Besides, the luminance $>100,000 \text{ cd m}^{-2}$ [40], color rendering index (CRI) >90 [41–46], correlated color temperature (CCT) mimicking sunlight (2500–8000 K) [47–49], and extremely stable color without variation of Commission International de L'Eclairage (CIE) chromaticity coordinates for WOLEDs have also been investigated [50–52]. Hence, these superior properties have demonstrated the great potential of the WOLED technology in the application of displays and lighting.

For the real commercialization, the lifetime is an essential parameter for WOLEDs (i.e., $\geq 10,000 \text{ h}$ at $\geq 1000 \text{ cd m}^{-2}$), aside from the general target for the PE of $40\text{--}70 \text{ lm W}^{-1}$ [53–58]. In the case of fluorescent WOLEDs, their lifetime could overtake $150,000 \text{ h}$ at 1000 cd m^{-2} [59]. However, the EQE, current efficiency (CE) and PE are unsatisfactory. To boost the lifetime and efficiency simultaneously, the introduction of tandem device architectures is very helpful [60–64]. This is because the lifetime of tandem OLEDs can be N-fold (N, the number of electroluminescent (EL) units) enhanced, since N-fold luminance can be achieved with the current density similar to that of single-unit OLEDs [65–68]. As a consequence, the EQE and CE can be also N-fold improved. With the careful manipulation of charge generation layers (CGLs), the PE is possible to be increased [69–71]. Therefore, tandem OLEDs have aroused both academic and industry interest. In 2005, Ma et al. reported the first tandem WOLEDs, where the CE and brightness equal basically to the sum of the two EL units [72]. Since then, a large number of endeavors have been taken to tandem WOLEDs [73–77]. As a matter of fact, the current commercial WOLEDs are almost based on tandem architectures. With the development of tandem WOLEDs, the fluorescent, phosphorescent and TADF emitters have been well connected with CGLs to realize desirable performance.

Herein, the fundamental concepts of tandem device architectures and their use in WOLEDs will be firstly described. Then, the state-of-the-art strategies to achieve high-performance tandem WOLEDs in recent years will be summarized. Specifically, the research progresses in the four types of tandem WOLEDs (i.e., tandem fluorescent WOLEDs, tandem phosphorescent WOLEDs, tandem TADF WOLEDs, and tandem hybrid WOLEDs) will be highlighted. Furthermore, doping-free tandem WOLEDs will be introduced. Finally, an outlook for the future development of tandem WOLEDs will be presented.

2. Fundamental Concepts of Tandem WOLEDs

2.1. The Device Architecture of Tandem OLEDs

To furnish white emissions, complementary-color emitters, three-color emitters or four-color emitters (e.g., blue/yellow, blue/orange, blue/red, blue/green/red, blue/yellow/red, blue/green/yellow/red) are commonly required [78–85]. For single-unit WOLEDs, the emitting layers (EMLs) can be composed of single or multiple EMLs. In general, single-EML WOLEDs only need one EML comprised of a versatile host doped with different color guests, while multiple-EML WOLEDs require at least two EMLs to produce white emissions [86–91]. Accordingly, the EL unit of tandem WOLEDs could be comprised of non-white or monochromatic EMLs, where various-color EMLs are located in different EL unit to combine for the white emission (type-I tandem WOLED architecture), as shown in Figure 1a. Besides, each unit of tandem of WOLEDs can be made up of multiple-EML white unit (type-II tandem WOLED architecture, Figure 1b) or single-EML white unit (type-III tandem WOLED architecture, Figure 1c). Alternatively, two unit-based tandem WOLEDs can be constructed by a white unit and a non-white unit (type-IV tandem WOLED architecture, Figure 1d). Based on the above facts, highly efficient phosphorescent and TADF emitters are usually adopted in tandem WOLEDs, which is expected to harvest both singlet and triplet excitons for the high performance [92–97]. After the optimization of EMLs, CGLs are selected to interconnect each EL unit.

As a result, tandem WOLEDs will be formed. It is deserved to note that most of tandem WOLEDs are focused on two or three EL units, although more than four units can be connected with CGLs.

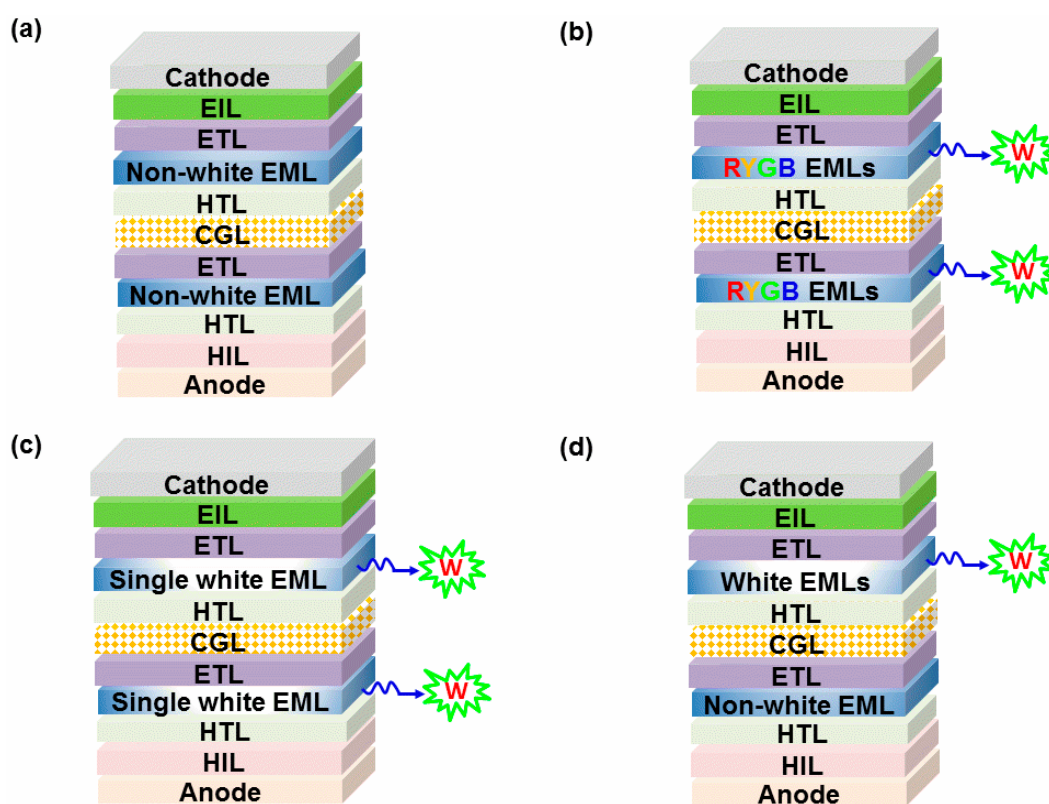


Figure 1. Typical device architectures for tandem white organic light-emitting diodes (WOLEDs). (a) Type-I tandem WOLED architecture, in which the white emission is generated via the combination of nonwhite or monochromatic emission from each electroluminescent (EL) unit. (b) Type-II tandem WOLED architecture, where RYGB emitting layers (EMLs) mean that more than two EMLs generating white emission in each EL unit. (c) Type-III tandem WOLED architecture, where each EML of the EL unit is single white EML. (d) Type-IV tandem WOLED architecture, where the non-white EML unit is combined with single white EML or RYGB EMLs. W is white emission, HIL is hole injection layer, HTL is hole transport layer, ETL is electron transport layer, EIL is electron injection layer.

2.2. The Role of Charge Generation Layer

To guarantee the high performance, the CGL plays a vital role in tandem WOLEDs, apart from the efficient each EL unit [98–100]. In 2003, Kido et al. reported the first tandem OLED by using n-doped organic/transparent conductive layer (i.e., Cs:2,9-dimethyl-4,7-diphenyl-1,10-phenanthroline (BCP)/indium tin oxide (ITO)) and n-doped organic/insulating materials (Cs:BCP/V₂O₅ or Cs:BCP/4F-TCNQ) as the CGLs [98]. Since then, numerous effective CGLs have been demonstrated. Briefly, a CGL acts as internal anode as well as cathode to generate charges and separate the opposite charges injecting to nearby EL unit [101]. Hence, tandem OLEDs can possibly convert one injected electron to multiple photons, obtaining higher luminance and CE at low current density. Such effect is beneficial to prolong the lifetime due to the avoidance of current leakage and breakdown caused by electric field [102–105].

For the formation of a CGL, a n-p semiconductor heterojunction is typically needed for the charge generation, which is located at the interface of n-type and p-type layers [106–110]. Besides, some demands are required for an efficient CGL, including excellent charge generation, small barrier for charge separation and injection into the nearby EL unit, outstanding transparency for visible emissions (e.g., $\geq 75\%$), good conductivity and long working stability [111–113]. So far, a large number

of CGLs have been put forward. Apart from the above mentioned n-doped organic material/metal oxide CGL [98], n-doped organic material/p-doped organic material CGL (e.g., Li:tris(8-quinolinolato) aluminum(III) (Alq_3)/ FeCl_3 :4,4'-N,N'-bis[N-(1-naphthyl)-N-phenylamino]biphenyl (NPB) [66], 4,7-diphenyl-1,10-phenanthroline (BPhen): Rb_2CO_3 /NPB: ReO_3 [114], Bphen: Rb_2CO_3 / ReO_3 /NPB: ReO_3 [114]) and organic heterojunction CGL (e.g., copper hexadecafluorophthalocyanine (F16CuPc)/copper phthalocyanine (CuPc) [115], fullerene (C60)/pentacene [116], zinc phthalocyanine (ZnPc):C60 [117]) are the most popular types.

In the physical processes of CGLs, charge generation and charge separation are the two main features. Hence, upon charges generating at the n-p junction, electrons and holes should be rapidly injected into nearby EL unit. To guarantee such charge separation, the CGL materials with high charge mobility or conductivity are ideal [118–122]. Besides, the energy barrier between CGLs and ETL or HTL in each EL unit should be minimized, which cannot only increase the charge injection into the EL unit but also reduce the charge accumulation [123–126]. To enhance the PE, the CGL is required to possess outstanding charge generation as well as charge separation. Particularly, negligible voltage drop across the CGL in the process of charge generation is required, otherwise the PE cannot be largely enhanced. This is because the voltage of tandem OLEDs usually increases N-fold compared with single-unit devices, leading to the fact that the PE of tandem OLEDs is similar to that of single-unit OLEDs.

3. Strategies for Tandem WOLEDs

3.1. Basic Aspects of Tandem WOLEDs

Based on the employed emitters, tandem WOLEDs can be classified into four types, i.e., tandem fluorescent WOLEDs, tandem phosphorescent WOLEDs, tandem TADF WOLEDs, and tandem hybrid WOLEDs. Thus, the selection of efficient emitters is essential to the high performance [127–132]. Unlike single-unit WOLEDs, the adoption of effective CGLs is another essential for high-performance tandem WOLEDs according to the above mentioned concepts. Therefore, the core features of strategies for tandem WOLEDs are the simultaneous management of efficient emitters and effective CGLs. To ensure the efficient emission can be produced in each EL unit of tandem WOLEDs, the careful manipulation of charges and excitons distribution is necessary [133–138]. Specifically, the issues of charge injection from the electrodes, charge transport and charge balance in EMLs, exciton generation, exciton harvesting, exciton recombination, exciton diffusion and exciton quenching should be well manipulated [139–142]. On the other hand, the CGL should not only be effective to generate and separate charges but also be able to optimize the optical effect to reduce the light loss. In the following sections, the design strategy, device architecture, emission mechanism as well as the effect of CGL in tandem WOLEDs have been highlighted, including tandem fluorescent, phosphorescent, TADF and hybrid WOLEDs. Additionally, the application of doping-free technique in tandem WOLEDs has also been described.

3.2. Tandem Fluorescent WOLEDs

The first tandem WOLED was based on fluorescent emitters, in which 4-(dicyanomethylene)-2-t-butyl-6-(1,1,7,7-tetramethyljulolidyl-9-enyl) 4H-pyran (DCJTb), Alq_3 and 9,10-bis-(β -naphthyl)-anthrene (ADN) were used as the red (600 nm), green (505 nm) and blue (435 nm) fluorescent emitter, respectively [72]. The device structure was ITO/NPB (50 nm)/ADN (30 nm)/BCP (10 nm)/ Alq_3 (40 nm)/BCP:Li (10 nm)/ V_2O_5 (30 nm)/NPB (50 nm)/ Alq_3 :DCJTb (40 nm)/ Alq_3 (40 nm)/LiF (1 nm)/Al (200 nm), which can be classified into type-I tandem WOLED architecture, as shown in Figure 2. As a result, the tandem WOLED showed a stable white light with CIE coordinates from (0.35, 0.32) at 18 V to (0.36, 0.36) at 50 V. The maximum luminance of 10,200 cd m^{-2} and CE was 10.7 cd A^{-1} , which were equal basically to the sum of the two EL units. For the origin of strikingly enhanced performance, the CGL of BCP:Li (10 nm)/ V_2O_5 (30 nm) played a key role. In brief, electrons and holes were generated within the CGL and then reached nearby Alq_3 and NPB, respectively. On one hand, these electrons could arrive at the blue EML ADN to

recombine with holes injected from anode, generating blue emission. Since BCP is a hole-blocking material, the holes distribution could be manipulated by adjusting the thickness of BCP layer, assuring blue and green emissions. On the other hand, holes generated from the CGL could reach the red EML Alq₃:DCJTb and recombine with electrons injected from cathode, producing the red emission. Therefore, white emission has been achieved.

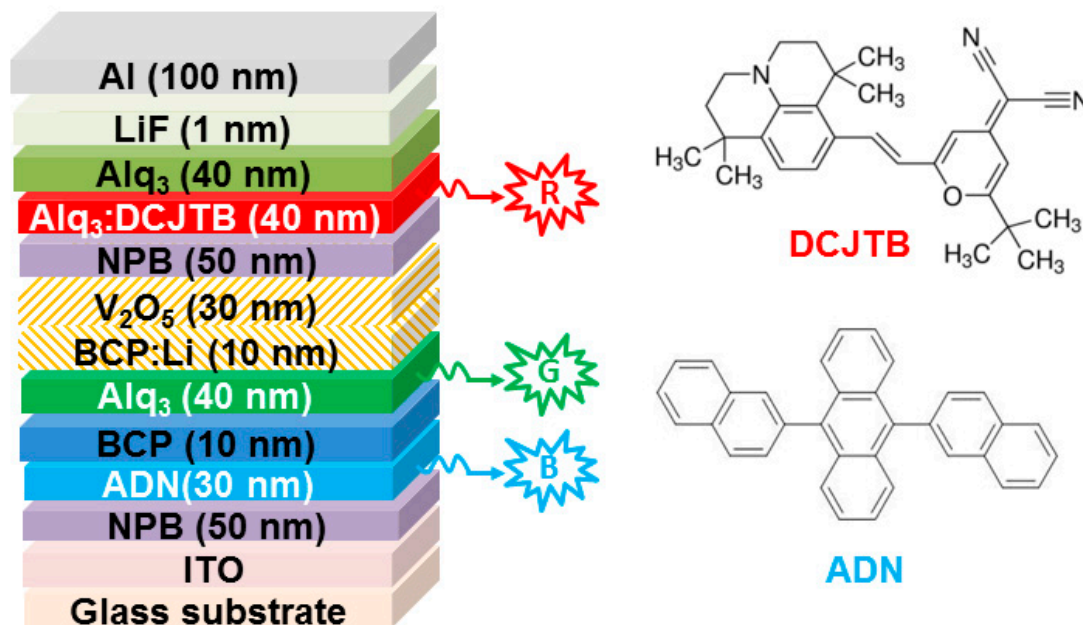


Figure 2. Right: the device structure of tandem WOLEDs. R, G and B represent red, green and blue emission, respectively. Left: the molecular structures of 4-(dicyanomethylene)-2-t-butyl-6-(1,1,7,7-tetramethyljulolidyl-9-enyl) 4H-pyran (DCJTb) and 9,10-bis-(β-naphthyl)-anthrene (AND) [72].

After Ma's pioneering work [72], many efforts have been made on tandem fluorescent WOLEDs [143]. For example, Ho et al. used n-doped organic material/p-doped organic material CGL (i.e., Bphen:2% cesium carbonate (Cs₂CO₃)/NPB:50% *v/v* tungsten oxide (WO₃)) to interconnect blue fluorescent EL unit and red fluorescent EL unit (type-I tandem WOLED architecture) [144]. By virtue of the p-i-n technology, their device showed a CE of 23.9 cd A⁻¹ and PE of 7.8 lm W⁻¹, which are one of the best for tandem fluorescent WOLEDs. However, despite the luminance and efficiency of tandem fluorescent WOLEDs can be scale linearly with the number of EL units, triplet excitons still decay nonradiatively, leading to the fact that the performance of this kind of devices is not satisfactory enough [145–149]. Therefore, more works are focused on phosphorescent or TADF emitters-based tandem WOLEDs.

3.3. Tandem Phosphorescent WOLEDs

In the case of phosphorescent emitters, triplet excitons can be harvested via the triplet-triplet energy transfer, while singlet excitons are harnessed via the singlet-triplet intersystem crossing process due to the heavy-atom effect, leading to a maximum IQE of 100% [150]. As an excellent result, single-unit phosphorescent WOLED with fluorescent tube efficiency has been demonstrated [151]. With the improvement of material design and device engineering, it is not very surprising to see that the EQE of single-unit phosphorescent WOLED can be >20% currently [152–154]. By extending the application of phosphorescent emitters into tandem WOLEDs, high-performance devices can be also developed with the management of effective CGLs.

In 2006, Kanno et al. reported the first tandem phosphorescent WOLED [155]. By using a n-doped organic material/metal oxide CGL (i.e., Bphen:Li/MoO₃) to interconnect the double-EML

white EL unit (i.e., 10 wt. fac-tris(1-(9,9-dimethyl-2-fluorenyl)pyrazolyl-*N,C2'*)iridium(III) (Ir(flz)₃):*N,N'*-dicarbazolyl-3,5-benzene (mCP, 20 nm)/10 iridium(III) bis(2-phenylquinolyl-*N,C2'*)acetylacetonate (PQIr):3 fac-tris(2-phenylpyridinato-*N,C2'*)iridium(III) (Ir(ppz)₃):4,4'-*N,N'*-dicarbazole-biphenyl (CBP, 5 nm)), tandem WOLEDs with 2 and 3 EL units were developed, which can be classified into type-II tandem WOLED architecture, as shown in Figure 3. As a result, the tandem WOLED with 3 EL units reached a peak forward-viewing EQE of 34.9% and total EQE of 51.0% at 500 cd m⁻². Briefly, there were four factors for the high performance. (i) The Li doping of Bphen in the CGL allowed for efficient electron injection, otherwise inefficient charge generation would occur. (ii) Charges and excitons were confined within the EMLs of each subpixel in the stack, by using materials with wide energy gaps i.e., fac-tris(1-phenylpyrazolyl-*N,C2'*)iridium(III) (Ir(ppz)₃) and Bphen as barriers to exciton and charge diffusion across the EML/HTL and EML/ETL interfaces, respectively. (iii) All exciton formation occurred within each EML by direct excitation of the triplet, either by injection from the lowest unoccupied molecular orbital (LUMO) CBP or by electron transfer from the mCP LUMO. (iv) Optical interference and weak microcavity effects were controlled by varying the thickness of HTL 4,4'-bis[*N*-(1-naphthyl)-*N*-phenyl-amino]biphenyl (NPD) with high hole mobility, since its thickness variation (<100 nm) would not significantly affect the voltage nor charge balance and hence the position of the recombination zone. Therefore, the charge confining structure and the effective CGL ensured a uniform white color balance for each subpixel, along with high efficiency for charge injection.

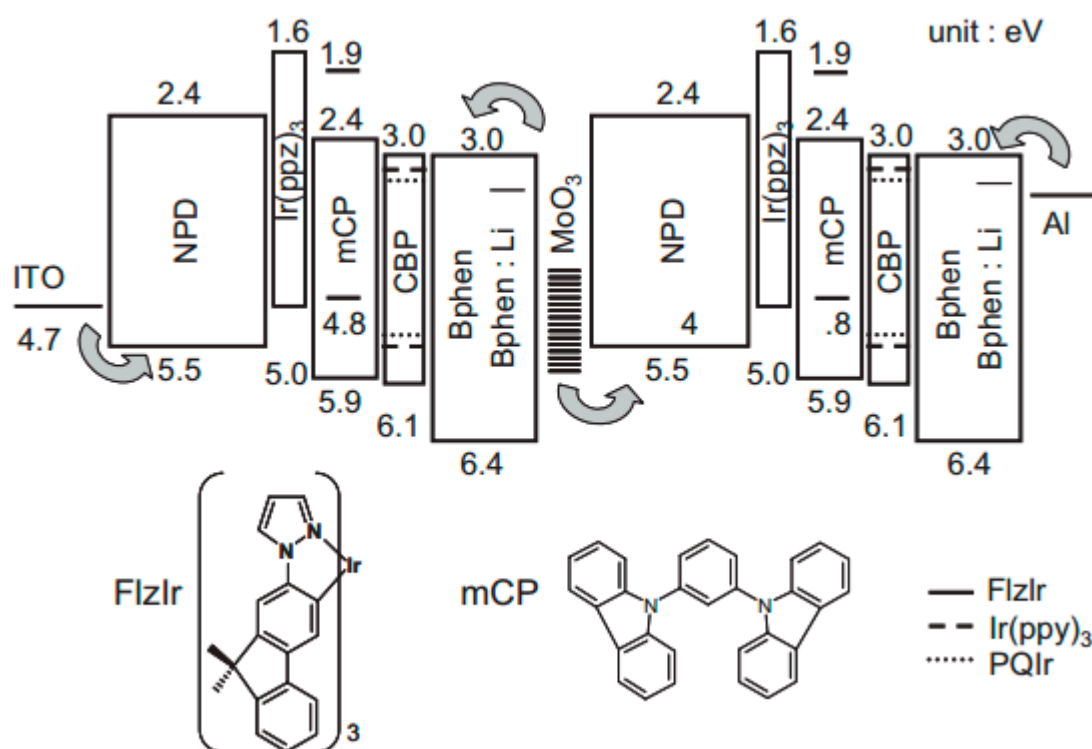


Figure 3. Top: Proposed energy-level diagram of tandem WOLEDs. Numbers indicate the HOMO and LUMO energies relative to vacuum. The arrows indicate the carrier injection from electrodes and the MoO₃ CGL. **Bottom:** The molecular structures of Ir(flz)₃ and mCP. Reproduced from reference [155].

In general, the architecture of type-III tandem WOLEDs is simpler than that of type-II tandem WOLEDs due to the reduced number of EMLs. However, it is usually more challenging to achieve high efficiency for single-EML WOLEDs compared with multiple-EML WOLEDs [156–160]. To loosen this bottleneck, Wang et al. have first realized highly efficient single-unit WOLED with the EML of mCP:iridium(III)[bis(4,6-difluorophenyl)-pyridinato-*N,C20*]picolinate (FIrpic):bis(2-(9,9-diethyl-9*H*-fluoren-2-yl)-1-phenyl-1*H*-benzimidazol-*N,C3*)iridium(acetylacetonate) ((fbi)₂Ir(acac)), by harvesting

all excitons via two parallel channels: host-guest energy transfer for FIrpic and direct exciton formation following charge trapping for $(\text{fbi})_2\text{Ir}(\text{acac})$ [161]. Then, they have used such single-EML architecture as the EL unit of a tandem WOLED via the interconnection of a n-doped organic material/metal oxide CGL (i.e., Li-doped BCP/MoO₃), which can be classified into type-III tandem WOLED architecture, as shown in Figure 4 [162]. As a result, the tandem WOLED exhibited a maximum forward viewing CE of 110.9 cd A⁻¹, EQE of 43.3% and PE of 45.2 lm W⁻¹, which were the best for tandem WOLEDs with two EL units at that time. Thus, the high performance was attributed to the combination of effective single units and CGL.

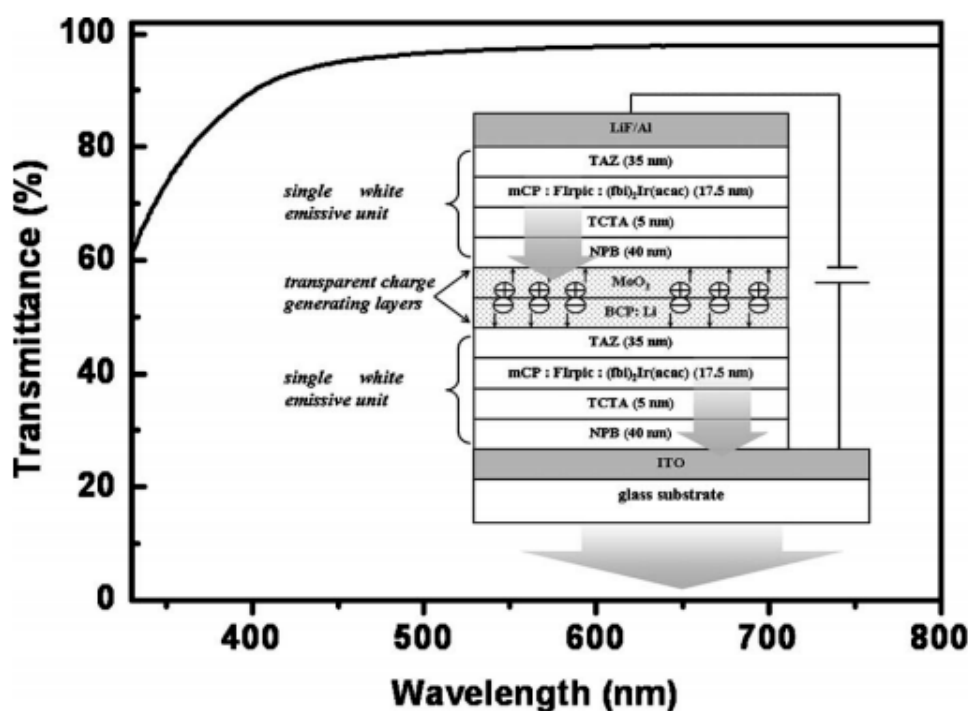


Figure 4. Transmittance spectrum of Li:BCP (10 nm)/MoO₃ (7 nm) thin film. **Inset:** schematic device structure of the tandem WOLED. Reproduced from reference [162].

After the selection of CGLs, the optimization of efficient phosphorescent emitters is key to the performance. Towards this end, Lee et al. used an exciplex-forming co-host and red- and green-phosphorescent dyes with horizontally oriented transition dipoles to optimize an orange OLED with a maximum EQE of 32% [163]. Next, by connecting such efficient orange EL unit with a blue phosphorescent EL unit via a CGL of Rb₂CO₃-doped BPhen/1,4,5,8,9,11-hexaazatriphenylene hexacarbonitrile (HATCN)/4,7-diphenyl-1,10-phenanthroline (TAPC), tandem WOLEDs showed a maximum EQE of 54.3% without outcoupling technology or EQE of 90.6% at 1000 cd m⁻² by attaching an index-matched glass half sphere onto the glass substrate. The device structure was ITO (70 nm)/4% ReO₃-doped mCP (x nm)/mCP (15 nm)/mCP:bis-4,6-(3,5-di-3-pyridylphenyl)-2-methylpyrimidine (B3PYMPM):FIrpic (15 nm, 0.7:0.3:0.057 molar ratio)/B3PYMPM (15 nm)/4 wt% Rb₂CO₃-doped B3PYMPM (25 nm)/23 wt% Rb₂CO₃-doped BPhen (10 nm)/HATCN (y nm)/TAPC (20 nm)/4,4',4''-tri(*N*-carbazolyl)triphen-ylamine (TCTA, 10 nm)/TCTA:B3PYMPM:iridium(III) bis(2-phenylquinoline) tetramethylheptadionate (Ir(ppy)₂(tmd)):Iridium(III) bis(4-methyl-2-(3,5-dimethylphenyl)quinolinato-*N,C2'*) tetramethylheptadionate (Ir(mphmq)₂(tmd)) (15 nm, 0.5:0.5:0.1:0.002 molar ratio)/B3PYMPM (60 nm)/LiF (0.7 nm)/Al (100 nm), which can be classified into type-I tandem WOLED architecture, as shown in Figure 5a. A key feature for the high performance was the introduction of the exciplex host TCTA:B3PYMPM for Ir(ppy)₂(tmd) and Ir(mphmq)₂(tmd) having highly oriented triplet transition dipole moments along the horizontal direction and high photoluminescence quantum yields (PLQY) [164–168]. Besides, the tandem device

architecture was optimized by an optical simulation to maximize the outcoupling of the emitted light. For example, the location for the blue EL unit, orange EL unit and the total thickness of ITO and organic layers have been optimized via the simulation based on the classical dipole model, as shown in Figure 5b–d.

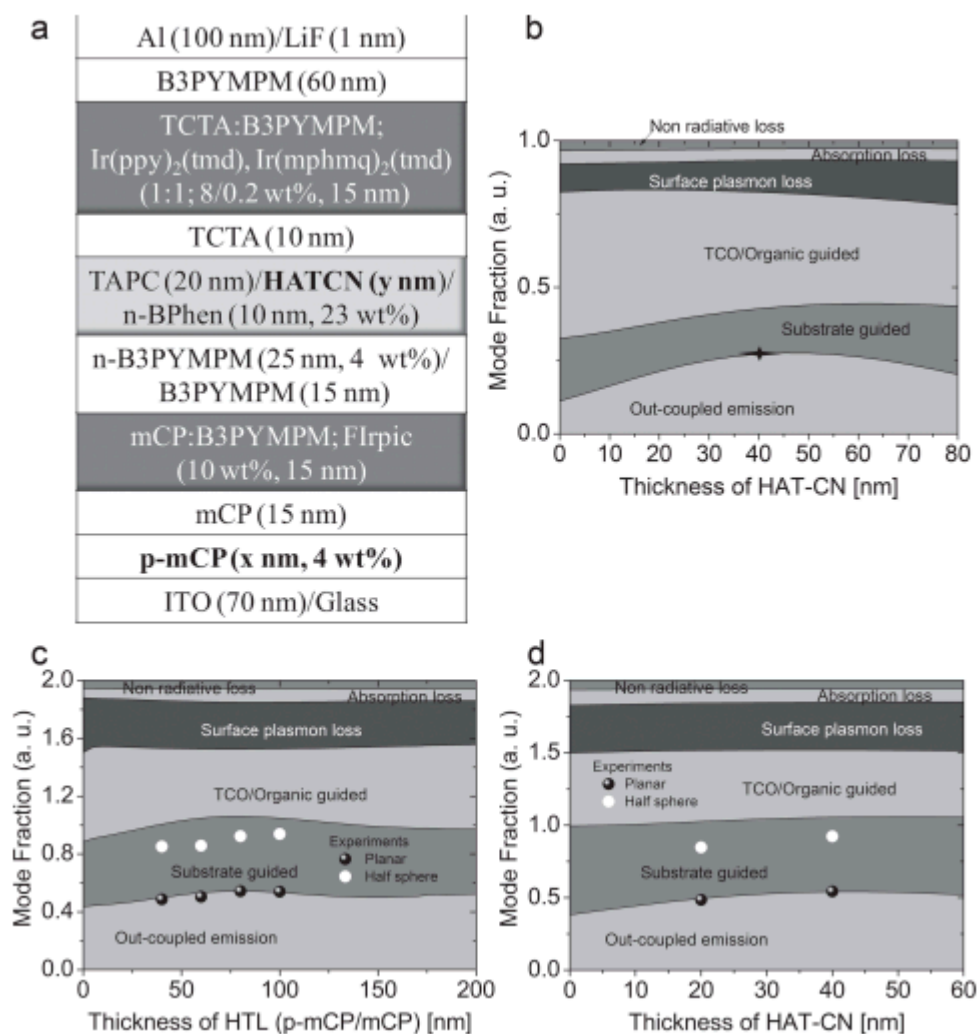


Figure 5. (a) Structure of tandem WOLEDs. (b) Mode analysis of blue light as a function of HATCN thickness with a total HTL thickness of 80 nm. \blackrightarrow indicates the thickness of HATCN when an out-coupled mode is maximized. (c) Mode analysis of white light as a function of the total HTL thickness at an HATCN thickness of 40 nm. (d) Mode analysis of white light as a function of HATCN thickness with a total HTL thickness of 80 nm. Reproduced from reference [163].

It is well-known that blue phosphorescent emitters usually exhibit poor stability [169–173]. Hence, the lifetime of tandem phosphorescent WOLEDs is limited. Recently, a strategy to address this issue has been proposed by Coburn et al. [174]. The device structure was glass substrate/150 nm ITO/10 nm HATCN/30 nm NPD/1-3 red-green emitter-CGL pairs (D3-D5, respectively)/blue element/CGL/red-green element/50 nm BPyTP2/1.5 nm 8-hydroxyquinolino lithium (LiQ)/100 nm Al, where the red-green element was 10 nm 4,40-bis(3-methylcarbazol-9-yl)-2,20-biphenyl (mCBP):8 vol % Ir(5'-Phppy)₃:10 vol % PQIr/25 nm mCBP:9 vol % Ir(5-Ph-ppy)₃/3 nm BALq/5 nm BALq:10 vol % PQIr/5 nm BALq, the blue element was 20 nm mCBP:18 → 14 vol % Ir(dmp)₃/10 nm mCBP:11 → 19 vol % Ir(dmp)₃:3 vol % mer-tris(*N*-phenyl, Nmethyl-pyridoimidazol-2-yl)iridium(III) (mer-Ir(pmp)₃)/20 nm mCBP:12 → 8 vol % Ir(dmp)₃/5 nm mCBP:8 vol % Ir(dmp)₃/5 nm mCBP/10 nm BPyTP2, the CGL was 8 nm 2,7-bis(2,20-bipyridine-5-yl)triphenylene (BPyTP2)/12 nm BPyTP2:3 vol %

Li/12 nm HATCN/5 nm NPD, D3, D4, and D5 indicated the total number of stacked elements separated by CGLs, as shown in Figure 6. As a result, the optimized tandem WOLED D5 showed a CCT of 2780 K, CRI of 89, a peak PE of 50 lm W^{-1} and a T_{70} lifetime (defined as the time corresponding to 30% decrease in luminance from an initial value of 1000 cd m^{-2}) of $80,000 \pm 2000 \text{ h}$, with minimal spectral shifts during aging. The key features for the high performance were red emissive blocking layers in the red-green element, graded doping and hot excited state management in the blue element, stable and low voltage CGLs, and effective outcoupling technique. More specifically, (i) stable bis(8-hydroxy-2-methylquinoline)-(4-phenylphenoxy)aluminum (BALq) was employed as a hole blocking layer for green element and a thin spacer between the green EML and red doped region, which could also reduce the loss of excitons transferred to its low triplet energy; (ii) the exciton confinement at the EML interface with NPD was obtained by doping red phosphor into a thin green EML adjacent to HTL; (iii) placing red EMLs on both sides of green EML reduced the color shift; (iv) dopant grading balanced hole and electron transport in blue EML, broadening the exciton recombination zone and reducing bimolecular annihilation rates that lead to molecular dissociation, which could increase the blue element stability; (v) mer-Ir(pmp)₃ was used to improve the reliability of the blue element by reducing the probability that hot excited states degrade host or emitter molecules; (vi) the CGL was stable and possessed high charge mobility; (vii) an outcoupling improvement of 2.2 ± 0.2 times over substrate emission by outcoupling substrate modes using index matching fluid between the device substrate and photodetector during the EQE measurement.

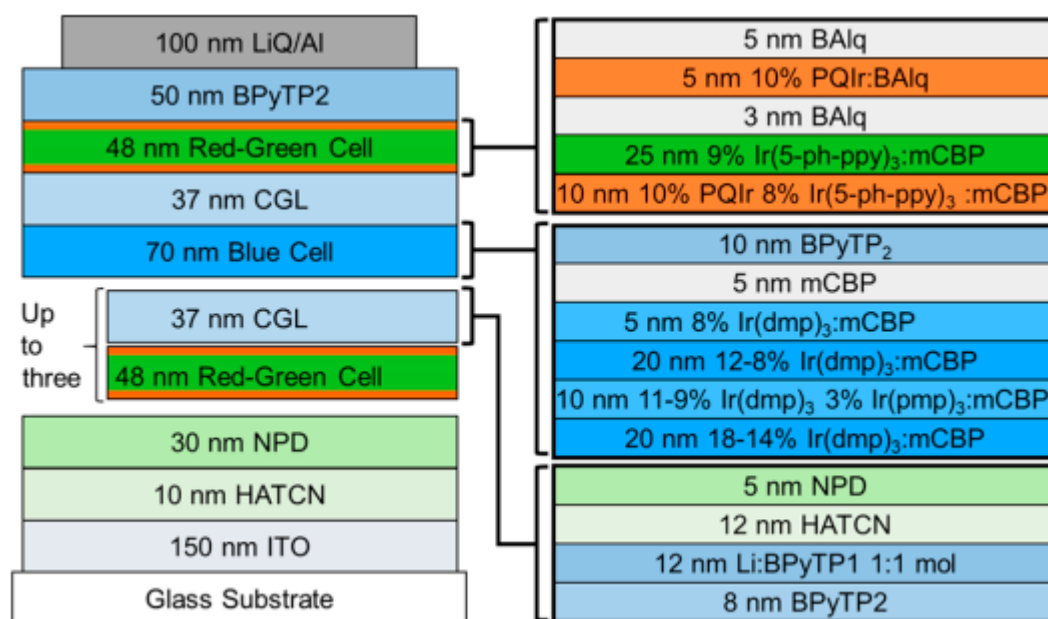


Figure 6. Device structure: (left) Tandem WOLEDs D3, D4, and D5 have one, two, and three CGL/red-green element pairs below the blue element, respectively. (Right) Layers of the red-green element, blue element and CGL. Reproduced from reference [174].

3.4. Tandem TADF WOLEDs

For TADF emitters, triplet excitons could be harnessed as delayed fluorescence through their up-conversion from a lowest triplet state to a lowest singlet state by inducing efficient reverse intersystem crossing [175–180]. Typically, the energy gap between T_1 and S_1 of $\leq 0.2 \text{ eV}$ is favorable to the thermal up-conversion [181–183]. Similar to phosphorescent emitters, 100% IQE can be attained for TADF emitters [184–186]. Thus, the excellent characteristics of TADF emitters render that they are promising for WOLEDs. Since the first single-unit TADF WOLED reported in 2014 [187], the EQE of TADF-based WOLEDs has been demonstrated to be as high as 20%, which is comparable to state-of-the-art phosphorescent WOLEDs [188–190]. So far, two kinds of TADF emitters have been

reported, TADF materials and TADF exciplexes [191–195]. In general, these two kinds of emitters can be used to develop high-performance WOLEDs by carefully manipulating the charges and excitons distribution [196].

By using effective CGLs to interconnect the TADF emitters (TADF materials or TADF exciplexes), tandem TADF WOLEDs can be achieved. Toward this target, Hung and coworkers demonstrated a tandem WOLED, in which blue TADF exciplex EL unit and yellow exciplex EL unit were interconnected by a CGL of 9,9-di[4-(di-p-tolyl)aminophenyl]fluorine (DTAF)/MoO₃/Al/Liq (holes and electrons were generated from the DTAF/MoO₃ interface) [197]. The structure was ITO/polyethylene dioxythiophene:polystyrene sulfonate (PEDOT:PSS, 30 nm)/TAPC (20 nm)/mCP (15 nm)/mCP:(1,3,5-triazine-2,4,6-triyl)tris(benzene-3,1-diyl)tris(diphenylphosphine oxide) (PO-T2T) (1:1, 20 nm)/PO-T2T (45 nm)/Liq (1 nm)/Al (1 nm)/MoO₃ (5 nm)/DTAF (20 nm)/DTAF:PO-T2T (1:1, 20 nm)/PO-T2T (50 nm)/Liq (0.5 nm)/Al (100 nm), as shown in Figure 7. As a result, an EQE of 11.6% was realized. For such high-efficiency exciplex based tandem WOLED, the efficient blue TADF exciplex is important. To accomplish this goal, Hung et al. synthesized PO-T2T having a low HOMO, low LUMO, high T₁ of 2.99 eV and electron mobility of >10⁻³ cm² V⁻¹ s⁻¹ as the acceptor. Combined with the mCP donor, the blue TADF exciplex emission could show an EQE of 8.0%, which ensured the high performance of tandem WOLED [188]. In Hung's device [197], the blue TADF exciplex has been used. To extend this strategy, Zhao et al. used a CGL of 2,4,6-tris(3-(1H-pyrazol-1-yl)phenyl)-1,3,5-triazine (3P-T2T):(Cs₂CO₃)/Al/MoO₃ to interconnect both blue TADF exciplex EL unit (TCTA:Bphen) and orange TADF exciplex unit (TAPC:2,4,6-tris(3-(1H-pyrazol-1-yl)phenyl)-1,3,5-triazine), achieving a tandem TADF WOLED with an EQE of 9.17% [198].

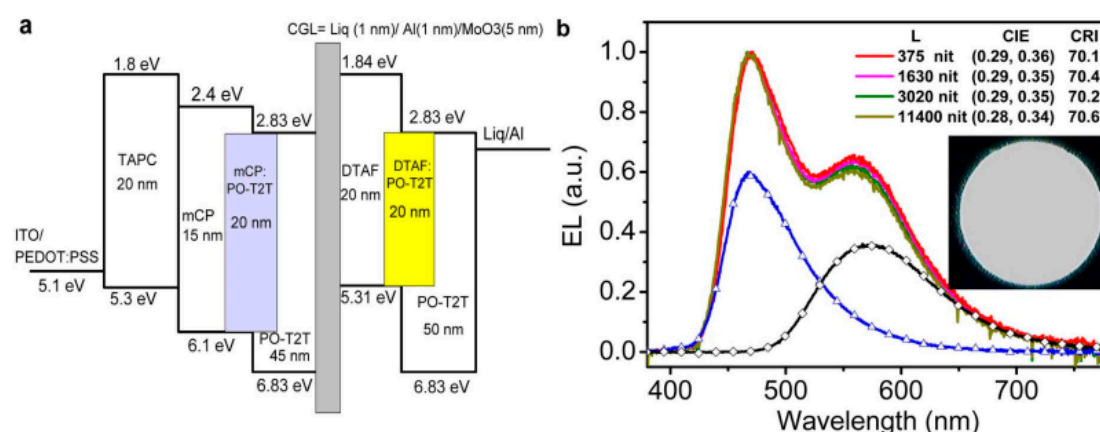


Figure 7. (a) Energy levels for the tandem WOLED. (b) EL spectra at various luminance, and two decomposed bands were blue and yellow exciplex emissions. Reproduced from reference [197].

3.5. Tandem Hybrid WOLEDs

With the combination of blue fluorescent/TADF emitters and green-red/yellow/orange phosphorescent emitters, hybrid WOLEDs can be achieved [199–205]. The first hybrid WOLED-based on blue fluorescent emitter was reported in 2003 [199]. Then, Sun et al. demonstrated the first efficient hybrid WOLED with a total EQE of 18.7% and a total PE of 37.6 lm W⁻¹ [200]. In 2014, Zhang et al. realized the first hybrid WOLED based on blue TADF emitter, achieving a maximum forward-viewing EQE of 22.5% and a peak PE of 47.6 lm W⁻¹ [55]. Due to the stable blue fluorescent emitters, most of available products in the WOLED market are adopted the hybrid WOLED technology. Particularly, tandem hybrid WOLEDs are promising for the practical applications.

To realize tandem hybrid WOLEDs, Kanno et al. used a CGL of Bphen:Li/MoO₃ to interconnect two hybrid white EL units [206]. Although this CGL was the same as that of their tandem phosphorescent WOLEDs [155], the tandem hybrid WOLED with three EL units showed

a maximum total EQE of 57% at a luminance of 1000 cd m⁻², representing a 25% increase relative their previous tandem phosphorescent WOLEDs [155]. For the origin of such high performance, an efficient management of singlet and triplet excitons has been accomplished in the EML of each white EL unit, by locating a CBP spacer between blue fluorescent emitting zone CBP:4,4'-bis(9-ethyl-3-carbazovinylen)-1,1'-biphenyl (BCzVBi) and the green and red phosphorescent regions containing CBP:Ir(ppy)₃ and CBP:PQIr, as shown in Figure 8. Therefore, BCzVBi harvested a majority of singlet excitons, with the remainder of lower energy triplets diffusing through the conductive host CBP to directly excite the green and red phosphors. Such structure allowed high PE via the resonant energy transfer from the conductive host into both the singlet and triplet energy levels. Besides, the NPD thickness in each EL unit was optimized to form the desired white balance in the presence of weak optical interference.

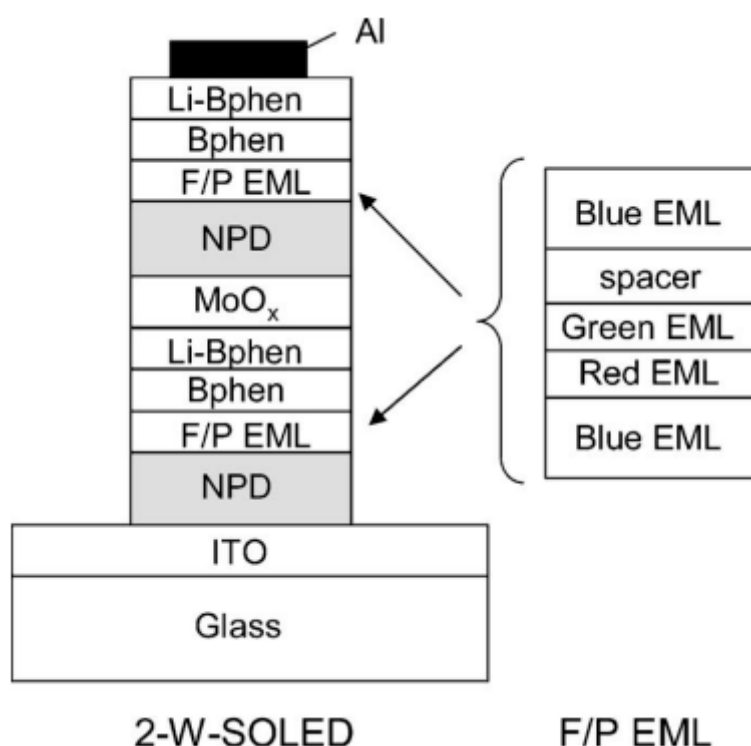


Figure 8. Structure of organic layers of a two-element WOLED. Reproduced from reference [206].

In Kanno's tandem hybrid WOLEDs, the T_1 of BCzVBi is lower than that of phosphorescent emitters. As a result, some triplet excitons are inevitably quenched by the high concentration of blue fluorophore, leading to the fact such device architecture is difficult to achieve 100% EQE [207–209]. To ensure the 100% IQE of tandem hybrid WOLEDs, Leo et al. proposed an effective strategy to develop tandem hybrid WOLEDs by using a CGL to interconnect the triplet-harvesting unit and mixed phosphorescent unit, as shown in Figure 9 [210]. In the triplet-harvesting unit, highly efficient fluorescent blue bulk emitter 4P-NPD was used as the blue emitter and host of red phosphorescent emitter Ir(MDQ)₂acac, since the T_1 of 4P-NPD (2.3 eV) is higher than that of Ir(MDQ)₂acac. Due to the p-type property of 4P-NPD, the structure of 65 nm HTL/10 nm Spiro-TAD/5 nm 4P-NPD:5 wt% Ir(MDQ)₂acac/5 nm 4P-NPD/10 nm BPhen/55 nm BPhen:Cs/100 nm Al rendered that a narrow recombination zone close to the hole blocking layer BPhen. By optimizing the thickness of undoped 4P-NPD layer to be larger than the extension of the recombination zone, Ir(MDQ)₂acac could only be excited by exciton diffusion owing to the different lifetimes of singlets and triplets (Figure 9). Therefore, the undoped 4P-NPD harvested the singlets, while Ir(MDQ)₂acac consumed the triplets, producing 100% IQE white emission. In the mixed phosphorescent unit, the structure of 50 nm HTL/10 nm Spiro-TAD/10 nm TCTA:8 wt% Ir(ppy)₃:1 wt% Ir(dhfp)₂acac/10 nm TPBi/50 nm BPhen:Cs/100 nm

Al ensured the green and yellow emissions from Ir(ppy)₃ and Ir(dhfpv)₂acac, respectively. The two phosphorescent emitters mixed in a common matrix TCTA were without loss of efficiency, which also reduced the voltage due to the reduction from two to one EML. As a consequence, both of the individual units had the ability to reach a 100% IQE. By stacking both units using a CGL consisting of a p/n-junction with a thin metal layer in between, the resultant architecture was 45 nm HTL (HTL1)/10 nm Spiro-TAD/5 nm 4P-NPD:5 wt% Ir(MDQ)₂acac/5 nm 4P-NPD/10 nm BPhen/90 nm BPhen:Cs(ETL1)/0.5 nm Al/85 nm HTL (HTL2)/10 nm Spiro-TAD/10 nm 8 wt% Ir(ppy)₃:1 wt% Ir(dhfpv)₂acac/10 nm TPBi/60 nm BPhen:Cs (ETL2)/100 nm Al. Thus, such device can be classified into type-IV tandem WOLED architecture. The PE and EQE were 33 lm W⁻¹ and 26%, respectively. Furthermore, by using a quadratic pyramid pattern and a high-refractive-index hemisphere to harvest all the light coupled into the substrate, silver cathode to reduce the absorption, optimized thickness of each transport layer, a PE of 90.5 lm W⁻¹ and EQE of 75.8% at 1000 cd m⁻² were obtained with the help of strongly increased light extraction. By extending this design strategy, Leo et al. have then developed efficient color stable inverted top-emitting tandem hybrid WOLEDs with ultra-thin wetting layer top electrodes [211], ITO-free tandem hybrid WOLEDs with angular color stability [212] and top-emitting tandem hybrid WOLEDs comprising laminated microlens films [213].

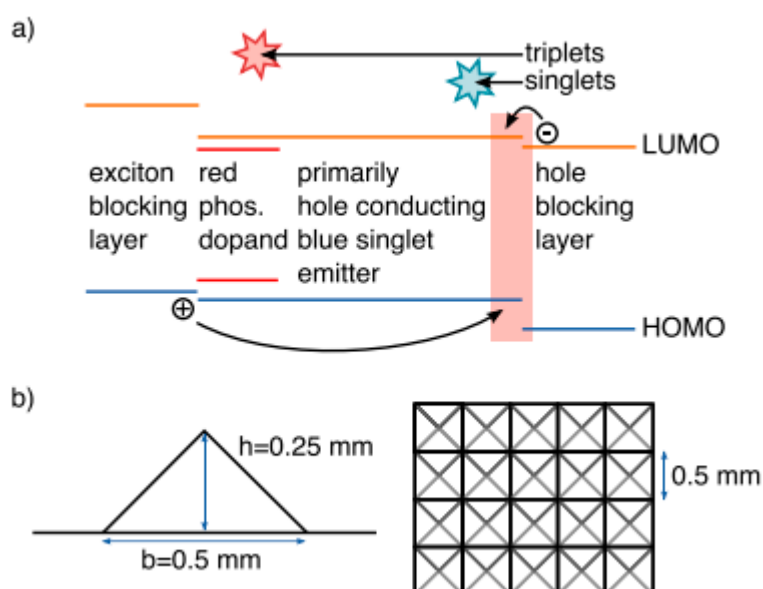


Figure 9. (a) Diffusively harvesting triplets. Due to the primarily hole-conducting character of 4P-NPD, excitons were formed close to Bphen. Whereas singlets recombine rapidly after creation, triplets diffuse to Ir(MDQ)₂acac. (b) Patterned surface for enhanced light extraction from the substrate. Reproduced from reference [210].

Since blue TADF emitters can produce highly efficient blue emission by harvest both singlet and triplet excitons, such kind of emitters have great potential to develop tandem hybrid WOLEDs [214,215]. Recently, Hung et al. reported the first tandem hybrid WOLED by utilizing blue TADF emitter bis[4-(9,9-dimethyl-9,10-dihydroacridine)phenyl]sulfone (DMAC-DPS) and orange phosphorescent emitter: bis(4-phenylthieno-[3,2-c]pyridine) (acetylacetonate)iridium(III) (PO-01), showing the peak CE of 78.5 cd A⁻¹ and EQE of 28.5% with the CIE coordinates of (0.33, 0.45) at 1000 cd m⁻² [216]. The device structure was ITO/HAT-CN (10 nm)/TAPC (40 nm)/TCTA (10 nm)/DMAC-DPS (20 nm)/DPEPO (5 nm)/TPBI (40 nm)/Bphen:Li (1.2, 15 nm)/HAT-CN (10 nm)/TAPC (40 nm)/TCTA (10 nm)/mCP:PO-01 (1.4, 20 nm)/1,3,5-tri[(3-pyridyl)-phen-3-yl] (TmPyPB, 40 nm)/Liq (2 nm)/Al (120 nm), as shown in Figure 10. Prior to the tandem hybrid WOLED, Hung et al. realized an efficient tandem green TADF OLED with the CGL of Bphen:Li/HAT-CN, achieving the EQE of 32.5%. Such results also demonstrated the CGL was effective, which was attributed to the efficient charge

generation, excellent optical transparency and good electron transporting properties of Bphen; Li. On the other hand, since both blue TADF emitter and phosphorescent emitter could harvest singlets and triplets in their individual EL unit, high efficiency was attained.

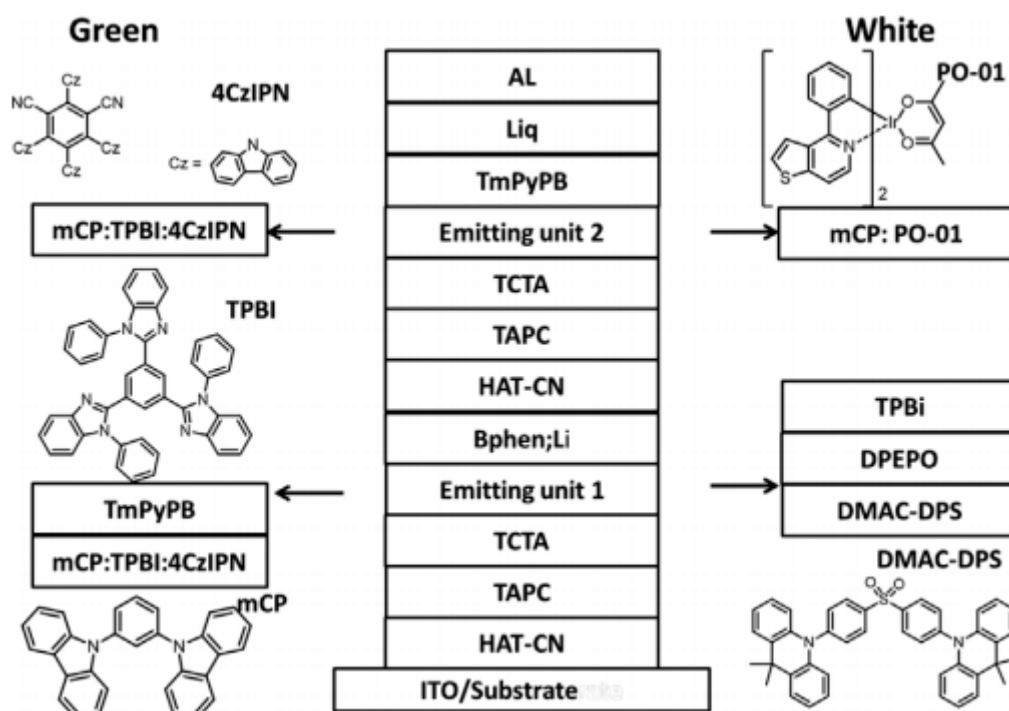


Figure 10. Device configurations of green (G1) and white (W1) OLEDs. Key molecular materials used for green emission (**left**) and those used for white emission (**right**) are shown. Reproduced from reference [216].

3.6. Doping-Free Tandem WOLEDs

Tandem WOLEDs can greatly boost the performance, however, their structures are intrinsically complicated compared with those of single-unit OLEDs. Additionally, the doping technology is required for high-performance tandem WOLEDs (e.g., the p-doping and n-doping charge transport layers, doping different-color EMLs, doping CGLs), which further complicating the structures [217–221]. To simplify the tandem WOLEDs, the doping-free technique may be conducive, since it can simplify the device engineering, shorten the fabrication procedure, avert the utilization of host and lower the cost [222–224].

In 2007, Liu et al. demonstrated the doping-free tandem WOLEDs by managing an effective doping-free CGL of Bepp₂ (25 nm) /KBH₄ (1 nm)/Ag (0.5 nm)/HAT-CN (130 nm)/NPB (15 nm) to interconnect doping-free EMLs and doping-free charge transport layers [224]. The device architecture was ITO/HAT-CN (100 nm)/NPB (15 nm)/TAPC (5 nm)/bis(2-phenyl-4,5-dimethylpyridinato)[2-(biphenyl-3-yl)pyridinato] iridium(III) (Ir(dmppy)₂(dpp), 0.6 nm)/CGL/TAPC (5 nm)/FIrpic (0.5 nm)/TmPyPB (50 nm)/LiF (1 nm)/Al (200 nm), where Ir(dmppy)₂(dpp) and FIrpic were the yellow and blue emitters (device W1), respectively, as shown in Figure 11. Additionally, by using the red emitter Ir(MDQ)₂(acac) to replace Ir(dmppy)₂(dpp) as well as optimizing the optical effect, another doping-free tandem WOLED was constructed (device W5). As a result, device W1 could accomplish the simplified structure/short fabrication time/reduced cost/high efficiency (81.2 cd A⁻¹)/low efficiency roll-off/low voltage/high luminance (44,886 cd m⁻²) trade-off, while device W5 could possess an acceptable CRI of 67. For the high performance, the doping-free CGL was effective to ensure the charge generation and separation. With the combination of KBH₄ and Ag to modify the Bepp₂/HAT-CN interface, the electron injection was improved, since metallic K was

released by the thermal decomposition of KBH_4 and the surface of Bepp_2 films was not an absolute plane. Hence, a thin K-doping Bepp_2 layer at the $\text{KBH}_4/\text{Bepp}_2$ interface was formed. Additionally, Ag functioned as electrodes for both units, also improving electron injection. On the other hand, phosphorescent emitters were adopted in each unit to not only harvest both singlet and triplet excitons but also ensure the white light.

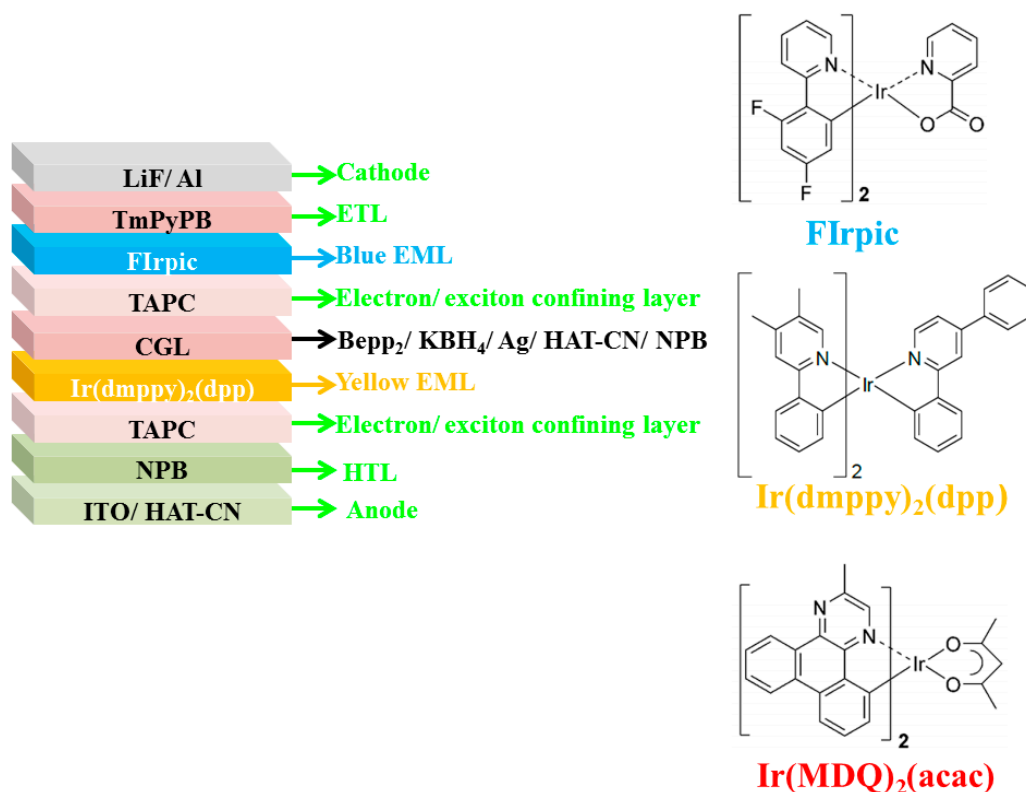


Figure 11. (Left): The structures of tandem WOLEDs. (Right): The chemical structure of used emitters. Reproduced from reference [224].

4. Summary and Outlook

Since tandem device architectures can impressively boost the luminance, efficiency and lifetime, the excellent characteristics render that tandem WOLED have been extensively investigated. In this review, we have mainly focused on recent developments in tandem WOLEDs and summarized the advanced strategies to achieve high-performance tandem WOLEDs. Particularly, we have emphasized representative tandem fluorescent WOLEDs, tandem phosphorescent WOLEDs, tandem TADF WOLEDs, and tandem hybrid WOLEDs. Additionally, we have also presented doping-free tandem WOLEDs. The detailed performances for tandem WOLEDs have been described in Table 1.

Table 1. Summarized performances for representative tandem WOLEDs.

WOLEDs ^a	V _{on} ^b (v)	EQE _{max} ^c (%)	PE _{max} ^d (lm W ⁻¹)	CE _{max} ^e (cd A ⁻¹)	CIE ^f	CRI ^g
Ref. [72]	-	-	2.6	10.7	(0.36, 0.34)	-
Ref. [155]	-	34.9	22.7	77.0	(0.35, 0.44)	66
Ref. [162]	-	43.3	45.2	110.9	(0.34, 0.41)	-
Ref. [163]	5.7	54.3	63	-	(0.359, 0.498)	-
Ref. [163] ^h	-	92.4	100	-	(0.336, 0.452)	-
Ref. [174]	-	74.3	24	-	(0.46, 0.43)	88.6
Ref. [174] ^h	-	171	50	-	(0.49, 0.43)	89.4
Ref. [197]	4.0	11.6	15.8	27.7	(0.29, 0.35)	70.6
Ref. [206]	-	33	14	-	(0.38, 0.44)	82
Ref. [210]	-	~26	~40	-	(0.505, 0.422)	77.6
Ref. [210] ^h	-	~78	~100	-	-	-
Ref. [216]	7.4	28.5	-	78.5	(0.33, 0.45)	82
Ref. [224]	5.1	-	81.2	42.9	(0.35, 0.47)	-

^a Representative tandem WOLEDs. ^b Turn-on voltage. ^c Peak EQE. ^d Peak PE. ^e Peak CE. ^f CIE coordinates at ~1000 cd m⁻². ^g Peak CRI. ^h With the use of outcoupling technique.

Over the past few years, the performance of tandem WOLEDs has incrementally enhanced and nowadays can satisfy the demand of real commercialization for handphones, lamps and televisions. In particular, phosphorescent and TADF emitters are favorable to increase the performance. To date, there are still many challenges hindering the further development of tandem WOLEDs, including the efficiency, driving voltage, operational stability as well as viewing angle dependence. First, the PE of tandem WOLEDs still lags behind. For example, the theoretical efficiency limit for WOLEDs is about 248 lm W⁻¹, indicating that there is still much room for tandem WOLEDs [225]. Besides, the voltage of tandem WOLEDs is much higher than that of single-unit WOLEDs, which increases the power consumption and easily leads to the low PE [226–228]. Therefore, each EL unit is required to harvest all excitons for efficient emission, while the CGL is needed to be effective for the charge generation and charge separation. In the internal physical processes, the elaborative management of the charge and exciton distribution is conducive. For the external procedures of light propagation, the utilization of outcoupling technologies can vastly enhance the efficiency as well as the lifetime [229–231]. This is because the use of light extraction layers can extract the light trapped by the substrate or the inner layers due to the total reflection. In addition, the light extraction layer (e.g., laminated microlens films) has been utilized to improve the CRI of tandem WOLEDs [214]. Therefore, although only a few outcoupling technologies were exclusively reported to enhance the performance of tandem WOLEDs, it is believed that the light extraction layers are promising for the further development of tandem WOLEDs. Additionally, the adoption of stable emitters and CGLs is also helpful to the lifetime.

Specifically, since the total thickness of tandem WOLEDs is very thick and the number of layers is large, the microcavity effect easily occurs because of the refractive index differences between adjacent layers (e.g., $n = 1.7$ for organic films, $n = 1.9$ for ITO, and $n = 2.2$ for MoO₃). Thus, tandem WOLEDs should have the Lambertian emission and the color should be stable over all angles (regardless of the center or the corner), otherwise chromaticity angular dependence will become a serious issue since the appearance of items can be rely on the locations [232]. Additionally, the device architecture of tandem WOLEDs is usually complicated. The introduction of a doping-free technique or solution-processed fabrication method is expected to be useful. After solving the aforementioned problems, the prospect of mass production for tandem WOLEDs will be possible and the proposed solutions are also beneficial to the related optoelectronic field (e.g., display, lighting, laser, solar cell, photodetectors and sensors) [233–238].

Author Contributions: P.X. and B.L. conceived the idea; P.X. and B.L. wrote the paper; J.H. and Y.Y. advised the paper; B.L. and Y.Y. supervised the project. All authors reviewed the paper.

Funding: The authors are grateful to the financial support from the National Natural Science Foundation of China (Grant Nos. 61804029, 11504050), Guangdong Natural Science Foundation (Grant No. 2018A030310353), Scientific

Research Starting Foundation of Foshan University (Grang No. Gg040926), Foshan Science and technology innovation special funds (Grant No. 2017EZ100111).

Conflicts of Interest: The authors declare no conflict of interest.

References

1. Yang, X.; Zhou, G.; Wong, W.-Y. Functionalization of Phosphorescent Emitters and Their Host Materials by Main-Group Elements for Phosphorescent Organic Light-Emitting Devices. *Chem. Soc. Rev.* **2015**, *44*, 8484–8575. [[CrossRef](#)] [[PubMed](#)]
2. Jou, J.-H.; Kumar, S.; Agrawal, A.; Li, T.-H.; Sahoo, S. Approaches for Fabricating High Efficiency Organic Light Emitting Diodes. *J. Mater. Chem. C* **2015**, *3*, 2974–3002. [[CrossRef](#)]
3. Liu, B.; Li, X.; Tao, H.; Zou, J.; Xu, M.; Wang, L.; Peng, J.; Cao, Y. Manipulation of Exciton Distribution for High-Performance Fluorescent/Phosphorescent Hybrid White Organic Light-Emitting Diodes. *J. Mater. Chem. C* **2017**, *5*, 7668–7683. [[CrossRef](#)]
4. Tyan, Y.S. Organic Light-Emitting-Diode Lighting Overview. *J. Photon. Energy* **2011**, *1*, 011009. [[CrossRef](#)]
5. Tang, C.W.; VanSlyke, V.A. Organic Electroluminescent Diodes. *Appl. Phys. Lett.* **1987**, *51*, 913. [[CrossRef](#)]
6. Fan, C.; Yang, C. Yellow/orange emissive heavy-metal complexes as phosphors in monochromatic and white organic light-emitting devices. *Chem. Soc. Rev.* **2014**, *43*, 6439–6469. [[CrossRef](#)]
7. Ma, Y.; Zhang, H.; Shen, J.; Che, C. Electroluminescence from triplet metal-ligand charge-transfer excited state of transition metal complexes. *Synth. Met.* **1998**, *94*, 245–248. [[CrossRef](#)]
8. Baldo, M.A.; O'Brien, D.F.; You, Y.; Shoustikov, A.; Sibley, S.; Thompson, M.E.; Forrest, S.R. Highly Efficient Phosphorescent Emission From Organic Electroluminescent Devices. *Nature* **1998**, *395*, 151–154. [[CrossRef](#)]
9. Liu, B.; Gao, D.; Wang, J.; Wang, X.; Wang, L.; Zou, J.; Ning, H.; Peng, J. Progress of White Organic Light-Emitting Diodes. *Acta Phys. Chim. Sin.* **2015**, *31*, 1823–1852.
10. Seifert, R.; Moraes, I.R.D.; Scholz, S.; Gather, M.C.; Lüssem, B.; Leo, K. Chemical Degradation Mechanisms of Highly Efficient Blue Phosphorescent Emitters Used for Organic Light Emitting Diodes. *Org. Electron.* **2013**, *14*, 115–123. [[CrossRef](#)]
11. Liu, B.; Xu, M.; Tao, H.; Ying, L.; Zou, J.; Wu, H.; Peng, J. Highly Efficient Red Phosphorescent Organic Light-Emitting Diodes Based on Solution Processed Emissive Layer. *J. Lumin.* **2013**, *142*, 35–39. [[CrossRef](#)]
12. Xiang, C.; Koo, W.; So, F.; Sasabe, H.; Kido, J. A Systematic Study on Efficiency Enhancements in Phosphorescent Green, Red and Blue Microcavity Organic Light Emitting Devices. *Light Sci. Appl.* **2013**, *2*, e74. [[CrossRef](#)]
13. Rao, M.V.M.; Su, Y.K.; Huang, T.S.; Chen, Y.C. White Organic Light Emitting Devices Based on Multiple Emissive Nanolayers. *Nano-Micro Lett.* **2010**, *2*, 242–246.
14. Eslamian, M. Inorganic and Organic Solution-Processed Thin Film Devices. *Nano-Micro Lett.* **2017**, *9*, 3. [[CrossRef](#)] [[PubMed](#)]
15. Burroughes, J.H.; Bradley, D.D.C.; Brown, A.R.; Marks, R.N.; Mackay, K.; Friend, R.H.; Burns, P.L.; Homes, A.B. Light-Emitting Diodes Based on Conjugated Polymers. *Nature* **1990**, *347*, 539–541. [[CrossRef](#)]
16. Uoyama, H.; Goushi, K.; Shizu, K.; Nomura, H.; Adachi, C. Highly Efficient Organic Light-Emitting Diodes from Delayed Fluorescence. *Nature* **2012**, *492*, 234–238. [[CrossRef](#)] [[PubMed](#)]
17. Nishimoto, T.; Yasuda, T.; Lee, S.Y.; Kondo, R.; Adachi, C. A Six-carbazole-decorated Cyclophosphazene as a Host with High Triplet Energy to Realize Efficient Delayed-Fluorescence OLEDs. *Mater. Horiz.* **2014**, *1*, 264–269. [[CrossRef](#)]
18. Zhang, Q.; Tsang, D.; Kuwabara, H.; Hatae, Y.; Li, B.; Takahashi, T.; Lee, S.Y.; Yasuda, T.; Adachi, C. Nearly 100% Internal Quantum Efficiency in Undoped Electroluminescent Devices Employing Pure Organic Emitters. *Adv. Mater.* **2015**, *27*, 2096–2100. [[CrossRef](#)] [[PubMed](#)]
19. Zhang, Q.S.; Li, B.; Huang, S.P.; Nomura, H.; Tanaka, H.; Adachi, C. Efficient blue organic light-emitting diodes employing thermally activated delayed fluorescence. *Nat. Photon.* **2014**, *8*, 326–332. [[CrossRef](#)]
20. Ying, L.; Ho, C.L.; Wu, H.; Cao, Y.; Wong, W.Y. White Polymer Light-Emitting Devices for Solid-State Lighting: Materials, Devices, and Recent Progress. *Adv. Mater.* **2014**, *26*, 2459–2473. [[CrossRef](#)]
21. Zou, J.; Wu, H.; Lam, C.S.; Wang, C.; Zhong, C.; Hu, S.; Ho, C.L.; Zhou, G.J.; Wu, H.; Choy, W.C.; et al. Simultaneous Optimization of Charge-Carrier Balance and Luminous Efficacy in Highly Efficient White Polymer Light-Emitting Devices. *Adv. Mater.* **2011**, *23*, 2976–2980. [[CrossRef](#)] [[PubMed](#)]

22. Niu, Y.H.; Liu, M.; Ka, J.W.; Bardeker, J.; Zin, M.; Schofield, Y.; Chi, Y.; Jen, A.K.-Y. Crosslinkable Hole-Transport Layer on Conducting Polymer for High-Efficiency White Polymer Light-Emitting Diodes. *Adv. Mater.* **2010**, *9*, 300–304. [[CrossRef](#)]
23. Wang, H.; Meng, L.Q.; Shen, X.X.; Wei, X.F.; Zheng, X.L.; Lv, X.P.; Yi, Y.P.; Wang, Y.; Wang, P.F. Light-Emitting Diodes: Highly Efficient Orange and Red Phosphorescent Organic Light-Emitting Diodes with Low Roll-Off of Efficiency using a Novel Thermally Activated Delayed Fluorescence Material as Host. *Adv. Mater.* **2015**, *27*, 4041–4047. [[CrossRef](#)]
24. Kim, B.S.; Lee, J.Y. Engineering of Mixed Host for High External Quantum Efficiency above 25% in Green Thermally Activated Delayed Fluorescence Device. *Adv. Funct. Mater.* **2015**, *24*, 3970–3977. [[CrossRef](#)]
25. Luo, D.X.; Yang, Y.B.; Huang, L.; Liu, B.; Zhao, Y. High-performance hybrid white organic light-emitting diodes exploiting blue thermally activated delayed fluorescent dyes. *Dyes Pigments* **2017**, *147*, 83–89. [[CrossRef](#)]
26. Sasabe, H.; Kido, J. Development of High Performance OLEDs for General Lighting. *J. Mater. Chem. C* **2013**, *1*, 1699–1707. [[CrossRef](#)]
27. Wang, Q.; Ma, D. Management of Charges and Excitons for High-performance White Organic Light-emitting Diodes. *Chem. Soc. Rev.* **2010**, *39*, 2387–2398. [[CrossRef](#)] [[PubMed](#)]
28. Chen, J.; Zhao, F.; Ma, D. Hybrid White OLEDs with Fluorophors and Phosphors. *Mater. Today* **2014**, *17*, 175–183. [[CrossRef](#)]
29. Zhang, L.; Li, X.-L.; Luo, D.; Xiao, P.; Xiao, W.; Song, Y.; Ang, Q.; Liu, B. Strategies to Achieve High-Performance White Organic Light-Emitting Diodes. *Materials* **2017**, *10*, 1378. [[CrossRef](#)]
30. Gather, M.C.; Reineke, S. Recent Advances in Light Outcoupling from White Organic Light-Emitting Diodes. *J. Photon. Energy* **2015**, *5*, 057607. [[CrossRef](#)]
31. Huang, H.; Yang, X.; Wang, Y.; Pan, B.; Wang, L.; Chen, J.; Ma, D.; Yang, C. Optimizing the conjugation between *N,N'*-dicarbazolyl-3,5-benzene and triphenylphosphine oxide as bipolar hybrids for highly efficient blue and single emissive layer white phosphorescent OLEDs. *Org. Electron.* **2013**, *14*, 2573–2581. [[CrossRef](#)]
32. Kido, J.; Hongawa, K.; Okuyama, K.; Nagai, K. White Light-Emitting Organic Electroluminescent Devices Using The Poly (*N*-vinylcarbazole) Emitter Layer Doped with Three Fluorescent Dyes. *Appl. Phys. Lett.* **1994**, *64*, 815. [[CrossRef](#)]
33. Kido, J.; Kimura, M.; Nagai, K. Multilayer White Light-Emitting Organic Electroluminescent Device. *Science* **1995**, *267*, 1332–1334. [[CrossRef](#)] [[PubMed](#)]
34. Ou, Q.D.; Zhou, L.; Li, Y.Q.; Chen, S.; Chen, J.D.; Li, C.; Wang, Q.K.; Lee, S.T.; Tang, J.X. Light-Emitting Diodes: Extremely Efficient White Organic Light-Emitting Diodes for General Lighting. *Adv. Funct. Mater.* **2014**, *24*, 7249. [[CrossRef](#)]
35. Liu, B.; Wang, L.; Xu, M.; Tao, H.; Gao, D.; Zou, J.; Lan, L.; Ning, H.; Peng, J.; Cao, Y. Extremely Stable-color Flexible White Organic Light-emitting Diodes with Efficiency Exceeding 100 lm W⁻¹. *J. Mater. Chem. C* **2014**, *2*, 9836. [[CrossRef](#)]
36. Liu, X.-K.; Zhan, C.; Jian, Q.; Wen-Jun, Z.; Bo, W.; Hoi Lam, T.; Zhu, F.; Zhang, X.-H.; Lee, C.-S. Organic light-emitting devices: Remanagement of singlet and triplet excitons in single-emissive-layer hybrid white organic light-emitting devices using thermally activated delayed fluorescent blue exciplex. *Adv. Mater.* **2015**, *27*, 7079–7085. [[CrossRef](#)]
37. Wu, Z.; Yu, L.; Zhao, F.; Qiao, X.; Chen, J.; Ni, F.; Yang, C.; Ahamad, T.; Alshehri, S.M.; Ma, D. Precise Exciton Allocation for Highly Efficient White Organic Light-Emitting Diodes with Low Efficiency Roll-Off Based on Blue Thermally Activated Delayed Fluorescent Exciplex Emission. *Adv. Opt. Mater.* **2017**, *5*, 1700415. [[CrossRef](#)]
38. Xiao, P.; Dong, T.; Xie, J.; Luo, D.; Yuan, J.; Liu, B. Emergence of White Organic Light-Emitting Diodes Based on Thermally Activated Delayed Fluorescence. *Appl. Sci.* **2018**, *8*, 299. [[CrossRef](#)]
39. Li, X.L.; Xie, G.Z.; Liu, M.; Chen, D.C.; Cai, X.Y.; Peng, J.B.; Cao, Y.; Su, S.J. High-Efficiency WOLEDs with High Color-Rendering Index based on a Chromaticity-Adjustable Yellow Thermally Activated Delayed Fluorescence Emitter. *Adv. Mater.* **2016**, *28*, 4614–4619. [[CrossRef](#)]
40. Liu, B.; Zou, J.H.; Zhou, Z.W.; Wang, L.; Xu, M.; Tao, H.; Gao, D.Y.; Lan, L.Y.; Ning, H.L.; Peng, J.B. Efficient single-emitting layer hybrid white organic light-emitting diodes with low efficiency roll-off, stable color and extremely high luminance. *J. Ind. Eng. Chem.* **2015**, *30*, 85–91. [[CrossRef](#)]

41. Sun, N.; Zhao, Y.B.; Zhao, F.C.; Chen, Y.H.; Yang, D.Z.; Chen, J.S.; Ma, D.G. A white organic light-emitting diode with ultra-high color rendering index, high efficiency, and extremely low efficiency roll-off. *Appl. Phys. Lett.* **2014**, *105*, 013303. [[CrossRef](#)]
42. Jou, J.-H.; Wu, R.-Z.; Yu, H.-H.; Li, C.-J.; Jou, Y.-C.; Peng, S.-H.; Chen, Y.-L.; Chen, C.-T.; Shen, S.-M.; Joers, P.; et al. Artificial Dusk-Light Based on Organic Light Emitting Diodes. *ACS Photon.* **2014**, *1*, 27–31. [[CrossRef](#)]
43. Jou, J.-H.; Hsieh, C.-Y.; Tseng, J.-R.; Peng, S.-H.; Jou, Y.-C.; Hong, J.H.; Shen, S.-M.; Tang, M.-C.; Chen, P.-C.; Lin, C.-H. Candle Light-Style Organic Light-Emitting Diodes. *Adv. Funct. Mater.* **2013**, *23*, 2750–2757. [[CrossRef](#)]
44. Shen, S.M.; Lin, C.R.; Wang, Y.S.; Chou, Y.C.; Chen, S.Z.; Jou, J.H. Efficient Very-High Color Rendering index Organic Light-Emitting Diode. *Org. Electron.* **2011**, *12*, 865–868.
45. Liu, B.; Xu, M.; Wang, L.; Tao, H.; Su, Y.; Gao, D.; Lan, L.; Zou, J.; Peng, J. Very-High Color Rendering Index Hybrid White Organic Light-Emitting Diodes with Double Emitting Nanolayers. *Nano-Micro Lett.* **2014**, *6*, 335–339. [[CrossRef](#)]
46. Liu, B.; Luo, D.; Gao, D.; Wang, X.; Xu, M.; Zou, J.; Ning, H.; Wang, L.; Peng, J.; Cao, Y. An ideal host-guest system to accomplish high-performance greenishyellow and hybrid white organic light-emitting diodes. *Org. Electron.* **2015**, *27*, 29–34. [[CrossRef](#)]
47. Jou, J.H.; Wu, M.H.; Shen, S.M.; Wang, H.C.; Chen, S.Z.; Chen, S.H.; Lin, C.R.; Hsieh, Y.L. Sunlight-Style Color-Temperature Tunable Organic Light-Emitting Diode. *Appl. Phys. Lett.* **2009**, *95*, 013307. [[CrossRef](#)]
48. Liu, B.; Nie, H.; Zhou, X.B.; Hu, S.B.; Luo, D.X.; Gao, D.Y.; Zou, J.H.; Xu, M.; Wang, L.; Zhao, Z.J.; et al. Manipulation of Charge and Exciton Distribution Based on Blue Aggregation-Induced Emission Fluorophors: A Novel Concept to Achieve High-Performance Hybrid White Organic Light-Emitting Diodes. *Adv. Funct. Mater.* **2016**, *26*, 776–783. [[CrossRef](#)]
49. Liu, B.; Nie, H.; Lin, G.; Hu, S.; Gao, D.; Zou, J.; Xu, M.; Wang, L.; Zhao, Z.; Ning, H.; et al. High-Performance Doping-Free Hybrid White OLEDs Based on Blue Aggregation-Induced Emission Luminogens. *ACS Appl. Mater. Interfaces* **2017**, *9*, 34162–34171. [[CrossRef](#)]
50. Liu, B.; Wang, L.; Gao, D.Y.; Xu, M.; Zhu, X.H.; Zou, J.H.; Lan, L.F.; Ning, H.L.; Peng, J.B.; Cao, Y. Harnessing charge and exciton distribution towards extremely high performance: The critical role of guests in single-emitting-layer white OLEDs. *Mater. Horiz.* **2015**, *2*, 536–544. [[CrossRef](#)]
51. Sun, N.; Wang, Q.; Zhao, Y.B.; Yang, D.Z.; Zhao, F.C.; Chen, J.S.; Ma, D.G. A hybrid white organic light-emitting diode with above 20% external quantum efficiency and extremely low efficiency roll-off. *J. Mater. Chem. C* **2014**, *2*, 7494–7504. [[CrossRef](#)]
52. Zhao, F.C.; Zhang, Z.Q.; Liu, Y.P.; Dai, Y.F.; Chen, J.S.; Ma, D. A Hybrid White Organic Light-Emitting Diode with Stable Color and Reduced Efficiency Roll-Off by Using a Bipolar Charge Carrier Switch. *Org. Electron.* **2012**, *13*, 1049–1055. [[CrossRef](#)]
53. Schwartz, G.; Reineke, S.; Rosenow, T.C.; Walzer, K.; Leo, K. Triplet Harvesting in Hybrid White Organic Light-Emitting Diodes. *Adv. Funct. Mater.* **2009**, *19*, 1319–1333. [[CrossRef](#)]
54. Zhang, D.D.; Duan, L.; Zhang, Y.G.; Cai, M.H.; Zhang, D.Q.; Qiu, Y. Highly efficient hybrid warm white organic light-emitting diodes using a blue thermally activated delayed fluorescence emitter: Exploiting the external heavy-atom effect. *Light Sci. Appl.* **2015**, *4*, e232. [[CrossRef](#)]
55. Zhang, D.D.; Duan, L.; Li, Y.L.; Zhang, D.Q.; Qiu, Y. Highly efficient and color-stable hybrid warm white organic light-emitting diodes using a blue material with thermally activated delayed fluorescence. *J. Mater. Chem. C* **2014**, *2*, 8191–8197. [[CrossRef](#)]
56. Zhang, D.D.; Zhang, D.Q.; Duan, L. Exploiting p-Type Delayed Fluorescence in Hybrid White OLEDs: Breaking the Trade-off between High Device Efficiency and Long Lifetime. *ACS Appl. Mater. Interfaces* **2016**, *8*, 23197–23203. [[CrossRef](#)]
57. Liu, B.; Wang, L.; Xu, M.; Tao, H.; Zou, J.H.; Gao, D.Y.; Lan, L.F.; Ning, H.L.; Peng, J.B.; Cao, Y. Efficient Hybrid White Organic Light-emitting Diodes with Extremely Long Lifetime: The Effect of n-type Interlayer. *Sci. Rep.* **2014**, *4*, 7198. [[CrossRef](#)] [[PubMed](#)]
58. Kim, G.H.; Lampande, R.; Im, J.B.; Lee, J.M.; Lee, J.Y.; Kwon, J.H. Controlling the exciton lifetime of blue thermally activated delayed fluorescence emitters using a heteroatom-containing pyridoindole donor moiety. *Mater. Horiz.* **2017**, *4*, 619–624. [[CrossRef](#)]

59. Duan, L.; Zhang, D.Q.; Wu, K.W.; Huang, X.Q.; Wang, L.D.; Qiu, Y. Controlling the Recombination Zone of White Organic Light-Emitting Diodes with Extremely Long Lifetimes. *Adv. Funct. Mater.* **2011**, *21*, 3540–3545. [[CrossRef](#)]
60. Yook, K.S.; Jeon, S.O.; Min, S.Y.; Lee, J.Y.; Yang, H.J.; Noh, T.; Kang, S.K.; Lee, T.W. Highly Efficient p-i-n and Tandem Organic Light-Emitting Devices Using an Air-Stable and Low-Temperature-Evaporable Metal Azide as an n-Dopant. *Adv. Funct. Mater.* **2010**, *20*, 1797–1802. [[CrossRef](#)]
61. Sun, H.D.; Guo, Q.X.; Yang, D.Z.; Chen, Y.H.; Chen, J.S.; Ma, D.G. High Efficiency Tandem Organic Light Emitting Diode Using an Organic Heterojunction as the Charge Generation Layer: An Investigation into the Charge Generation Model and Device Performance. *ACS Photon.* **2015**, *2*, 271–279. [[CrossRef](#)]
62. Ding, L.; Sun, Y.Q.; Chen, H.; Zu, F.S.; Wang, Z.K.; Liao, L.S. A novel intermediate connector with improved charge generation and separation for large-area tandem white organic lighting devices. *J. Mater. Chem. C* **2014**, *2*, 10403–10408. [[CrossRef](#)]
63. Chang, C.C.; Chen, J.F.; Hwang, S.W.; Chen, C.H. Highly efficient white organic electroluminescent devices based on tandem architecture. *Appl. Phys. Lett.* **2005**, *87*, 253501. [[CrossRef](#)]
64. Hong, T.; Gao, D.; Liu, B.; Wang, L.; Zou, J.; Xu, M.; Peng, J. Enhancement of Tandem Organic Light-Emitting Diode Performance by Inserting An Ultra-Thin Ag Layer in Charge Generation Layer. *Acta Phys. Sin.* **2017**, *1*, 017302.
65. Lei, D.; Tang, X.; Xu, M.F.; Shi, X.B.; Wang, Z.K.; Liao, L.S. Lithium Hydride Doped Intermediate Connector for High-Efficiency and Long-Term Stable Tandem Organic Light-Emitting Diodes. *ACS Appl. Mater. Interfaces* **2014**, *6*, 18228–18232.
66. Liao, L.S.; Klubek, K.P.; Tang, C.W. High-Efficiency Tandem Organic Light-Emitting Diodes. *Appl. Phys. Lett.* **2004**, *84*, 167–169. [[CrossRef](#)]
67. Liu, J.; Wang, J.; Huang, S.; Shi, X.; Wu, X.; He, G. A highly efficient, transparent and stable charge generation unit based on a p-doped monolayer. *Org. Electron.* **2013**, *14*, 1337–1343. [[CrossRef](#)]
68. Bao, Q.Y.; Yang, J.P.; Tang, J.X.; Li, Y.; Lee, C.S.; Lee, S.T. Interfacial Electronic Structures of WO₃-Based Intermediate Connectors in Tandem Organic Light-Emitting Diodes. *Org. Electron.* **2010**, *11*, 1578–1583. [[CrossRef](#)]
69. Liao, L.S.; Klubek, K.P. Power Efficiency Improvement in a Tandem Organic Light-Emitting Diode. *Appl. Phys. Lett.* **2008**, *92*, 223311. [[CrossRef](#)]
70. Yang, Y.; Peng, T.; Ye, K.Q.; Wu, Y.; Liu, Y.; Wang, Y. High-efficiency and high-quality white organic light-emitting diode employing fluorescent emitters. *Org. Electron.* **2011**, *12*, 29–33. [[CrossRef](#)]
71. Chen, Y.H.; Wang, Q.; Chen, J.S.; Ma, D.; Yan, D.H.; Wang, L.X. Organic Semiconductor Heterojunction as Charge Generation Layer in Tandem Organic Light-Emitting Diodes for High Power Efficiency. *Org. Electron.* **2012**, *13*, 1121–1128. [[CrossRef](#)]
72. Guo, F.; Ma, D. White organic light-emitting diodes based on tandem structures. *Appl. Phys. Lett.* **2005**, *87*, 173510. [[CrossRef](#)]
73. Lee, T.W.; Noh, T.; Choi, B.K.; Kim, M.S.; Shin, D.W. High-Efficiency Stacked White Organic Light-Emitting Diodes. *Appl. Phys. Lett.* **2008**, *92*, 43301. [[CrossRef](#)]
74. Yu, Y.; Chen, X.; Jin, Y.; Wu, Z.; Yu, Y.; Lin, W. Electron-Transporting Layer Doped With Cesium Azide for High-Performance Phosphorescent and Tandem White Organic Light-Emitting Devices. *J. Appl. Phys. D* **2017**, *50*, 275104. [[CrossRef](#)]
75. Shi, C.; Sun, N.; Wu, Z.; Chen, J.; Ma, D. High Performance Hybrid Tandem White Organic Light-Emitting Diodes by Using A Novel Intermediate Connector. *J. Mater. Chem. C* **2018**, *6*, 767–772. [[CrossRef](#)]
76. Kim, H.S.; Joo, C.W.; Pyo, B.; Lee, J.M.; Suh, C. Improvement of Viewing Angle Dependence of the White Organic Light Emitting Diodes With Tandem Structure by Introduction of Nanoporous Ppolymer Films. *Org. Electron.* **2017**, *40*, 88–96. [[CrossRef](#)]
77. Cho, H.; Song, J.; Kwon, B.H.; Choi, S.; Lee, H.; Joo, C.W.; Ahn, S.D.; Kang, S.Y.; Yoo, S.; Moon, J. Stabilizing Color Shift of Tandem White Organic Light-Emitting Diodes. *J. Ind. Eng. Chem.* **2018**, *69*, 414–421. [[CrossRef](#)]
78. Chen, Y.; Zhao, F.; Zhao, Y.; Chen, J.; Ma, D. Ultra-simple hybrid white organic light-emitting diodes with high efficiency and CRI trade-off: Fabrication and emission-mechanism analysis. *Org. Electron.* **2012**, *13*, 2807–2815. [[CrossRef](#)]

79. Zhao, Y.; Zhu, L.; Chen, J.; Ma, D. Improving Color Stability of Blue/Orange Complementary White OLEDs by Using Single-Host Double-Emissive Layer Structure: Comprehensive Experimental Investigation into the Device Working Mechanism. *Org. Electron.* **2012**, *13*, 1340–1348. [[CrossRef](#)]
80. Luo, D.X.; Yang, Y.F.; Xiao, Y.; Zhao, Y.; Yang, Y.B.; Liu, B.Q. Regulating Charge and Exciton Distribution in High-Performance Hybrid White Organic Light-Emitting Diodes with n-Type Interlayer Switch. *Nano-Micro Lett.* **2017**, *9*, 37–44. [[CrossRef](#)]
81. Liu, B.; Xu, M.; Wang, L.; Su, Y.J.; Gao, D.Y.; Tao, H.; Lan, L.F.; Zou, J.H.; Peng, J.B. High-Performance Hybrid White Organic Light-Emitting Diodes Comprising Ultrathin Blue and Orange Emissive Layers. *Appl. Phys. Express* **2013**, *6*, 122101. [[CrossRef](#)]
82. Poloek, A.; Chen, C.-T.; Chen, C.-T. High performance hybrid white and multi-colour electroluminescence from a new host material for a heteroleptic naphthyridinolate platinum complex dopant. *J. Mater. Chem. C* **2014**, *2*, 1376–1380. [[CrossRef](#)]
83. Schwartz, G.; Fehse, K.; Pfeiffer, M.; Walzer, K.; Leo, K. Highly efficient white organic light emitting diodes comprising an interlayer to separate fluorescent and phosphorescent regions. *Appl. Phys. Lett.* **2006**, *89*, 083509. [[CrossRef](#)]
84. Zhou, J.; Zou, J.; Dai, C.; Zhang, Y.; Luo, X.; Liu, B. High-Efficiency and High-Luminance Three-Color White Organic Light-Emitting Diodes with Low Efficiency Roll-Off. *ECS J. Solid State Sci. Technol.* **2018**, *7*, R99–R103. [[CrossRef](#)]
85. Huang, W.Y.; Chen, Z.W.; You, H.W.; Fan, F.C.; Chen, H.F.; Wong, K.T. Efficient carrier- and exciton-confining device structure that enhances blue PhOLED efficiency and reduces efficiency roll-off. *Org. Electron.* **2011**, *12*, 575–581. [[CrossRef](#)]
86. Zhang, B.; Tan, G.; Lam, C.S.; Yao, B.; Ho, C.L.; Liu, L.; Xie, Z.; Wong, W.Y.; Ding, J.; Wang, L. High-Efficiency Single Emissive Layer White Organic Light-Emitting Diodes Based on Solution-Processed Dendritic Host and New Orange-Emitting Iridium Complex. *Adv. Mater.* **2012**, *24*, 1873–1877. [[CrossRef](#)] [[PubMed](#)]
87. Yin, Y.; Piao, X.; Li, Y.; Wang, Y. High-Efficiency and Low-Efficiency-Roll-Off Single-Layer White Organic Light-Emitting Devices with a Bipolar Transport Host. *Appl. Phys. Lett.* **2012**, *101*, 063306. [[CrossRef](#)]
88. Chang, Y.L.; Song, Y.; Wang, Z.; Helander, M.G.; Qiu, J.; Chai, L.; Liu, Z.; Scholes, G.D.; Lu, Z. Highly Efficient Warm White Organic Light-Emitting Diodes by Triplet Exciton Conversion. *Adv. Funct. Mater.* **2013**, *23*, 705–712. [[CrossRef](#)]
89. Liu, B.; Luo, D.X.; Zou, J.H.; Gao, D.Y.; Ning, H.L.; Wang, L.; Peng, J.B.; Cao, Y. A host-guest system comprising high guest concentration to achieve simplified and high-performance hybrid white organic light-emitting diodes. *J. Mater. Chem. C* **2015**, *3*, 6359–6366. [[CrossRef](#)]
90. Ouyang, X.H.; Li, X.L.; Bai, Y.Q.; Mi, D.B.; Ge, Z.Y.; Su, S.J. Highly-efficient hybrid white organic light-emitting diodes based on a high radiative exciton ratio deepblue emitter with improved concentration of phosphorescent dopant. *RSC Adv.* **2015**, *5*, 32298–32306. [[CrossRef](#)]
91. Fleetham, T.; Huang, L.; Li, J. Tetradentate Platinum Complexes for Efficient and Stable Excimer-Based White OLEDs. *Adv. Funct. Mater.* **2015**, *24*, 6066–6073. [[CrossRef](#)]
92. Chen, P.; Xie, W.F.; Li, K.; Guan, T.; Duan, Y.; Zhao, Y.; Liu, S.Y.; Ma, C.S.; Zhang, L.Y.; Li, B. White organic light-emitting devices with a bipolar transport layer between blue fluorescent and orange phosphorescent emitting layers. *Appl. Phys. Lett.* **2007**, *91*, 023505. [[CrossRef](#)]
93. Liu, B.; Xu, M.; Tao, H.; Su, Y.J.; Gao, D.Y.; Zou, J.H.; Lan, L.F.; Peng, J.B. The effect of spacer in hybrid white organic light emitting diodes. *Chin. Sci. Bull.* **2014**, *59*, 3090–3097. [[CrossRef](#)]
94. Zou, J.; Liu, J.; Wu, H.; Yang, W.; Peng, J.; Cao, Y. High-Efficiency and Good Color Quality White Light-Emitting Devices Based on Polymer Blend. *Org. Electron.* **2009**, *10*, 843. [[CrossRef](#)]
95. Chen, D.; Xie, G.; Cai, X.; Liu, M.; Cao, Y.; Su, S.-J. Fluorescent Organic Planar pn Heterojunction Light-Emitting Diodes with Simplified Structure, Extremely Low Driving Voltage, and High Efficiency. *Adv. Mater.* **2016**, *28*, 239–244. [[CrossRef](#)]
96. Chen, D.; Wang, Z.; Wang, D.; Wu, Y.-C.; Lo, C.-C.; Lien, A.; Cao, Y.; Su, S.-J. Efficient Exciplex Organic Light-Emitting Diodes with a Bipolar Acceptor. *Org. Electron.* **2015**, *25*, 79–84. [[CrossRef](#)]
97. Wu, S.F.; Li, S.H.; Wang, Y.K.; Huang, C.C.; Sun, Q.; Liang, J.J.; Liao, L.S.; Fung, M.-K. White Organic LED with a Luminous Efficacy Exceeding 100 lm w⁻¹ without Light Out-Coupling Enhancement Techniques. *Adv. Funct. Mater.* **2017**, *27*, 1701314. [[CrossRef](#)]

98. Kido, J.; Matsumoto, T.; Nakada, T.; Endo, J.; Mori, K.; Kawamura, N.; Yokoi, A. Dig. 27.1: Invited Paper: High Efficiency Organic EL Devices having Charge Generation Layers. *J. Tech. Pap. Soc. Inf. Disp. Int. Symp.* **2003**, *34*, 964–965. [[CrossRef](#)]
99. Pu, Y.J.; Chiba, T.; Ideta, K.; Takahashi, S.; Aizawa, N.; Hikichi, T.; Kido, J. Fabrication of Organic Light-Emitting Devices Comprising Stacked Light-Emitting Units by Solution-Based Processes. *Adv. Mater.* **2015**, *27*, 1327–1332. [[CrossRef](#)]
100. Yu, J.; Yin, Y.M.; Liu, W.B.; Zhang, W.; Zhang, L.T.; Xie, W.F.; Zhao, H.Y. Effect of the greenish-yellow emission on the color rendering index of white organic light-emitting devices. *Org. Electron.* **2014**, *15*, 2817–2821. [[CrossRef](#)]
101. Chen, Y.H.; Ma, D. Organic semiconductor heterojunctions as charge generation layers and their application in tandem organic light-emitting diodes for high power efficiency. *J. Mater. Chem.* **2012**, *22*, 18718–18734. [[CrossRef](#)]
102. Kim, M.; Jeon, S.K.; Hwang, S.H.; Lee, J.Y. Stable Blue Thermally Activated Delayed Fluorescent Organic Light-Emitting Diodes with Three Times Longer Lifetime than Phosphorescent Organic Light-Emitting Diodes. *Adv. Mater.* **2015**, *27*, 2515–2520. [[CrossRef](#)] [[PubMed](#)]
103. Shi, Z.; Li, Y.; Li, S.; Li, X.; Wu, D.; Xu, T.; Tian, Y.; Chen, Y.; Zhang, Y.; Zhang, B.; et al. Localized Surface Plasmon Enhanced All-Inorganic Perovskite Quantum Dot Light-Emitting Diodes Based on Coaxial Core/Shell Heterojunction Architecture. *Adv. Funct. Mater.* **2018**, *28*, 1707031. [[CrossRef](#)]
104. Xiao, P.; Huang, J.; Yu, Y.; Yuan, J.; Luo, D.; Liu, B.; Liang, D. Recent Advances of Exciplex-Based White Organic Light-Emitting Diodes. *Appl. Sci.* **2018**, *8*, 1449. [[CrossRef](#)]
105. Liu, B.; Xu, M.; Wang, L.; Yan, X.; Tao, H.; Su, Y.; Gao, D.; Lan, L.; Zou, J.; Peng, J. Investigation and Optimization of Each Organic Layer: A Simple But Effective Approach Towards Achieving High-Efficiency Hybrid White Organic Light-Emitting Diodes. *Org. Electron.* **2014**, *15*, 926–936. [[CrossRef](#)]
106. Li, X.L.; Ouyang, X.H.; Liu, M.; Ge, Z.Y.; Peng, J.B.; Cao, Y.; Su, S.J. Highly efficient single-and multi-emission-layer fluorescent/phosphorescent hybrid white organic light-emitting diodes with ~20% external quantum efficiency. *J. Mater. Chem. C* **2015**, *3*, 9233–9239. [[CrossRef](#)]
107. Kim, D.Y.; Park, J.H.; Lee, J.W.; Hwang, S.; Oh, S.J.; Kim, J.; Sone, C.; Schubert, E.F.; Kim, J.K. Overcoming the fundamental light-extraction efficiency limitations of deep ultraviolet light-emitting diodes by utilizing transverse-magnetic-dominant emission. *Light Sci. Appl.* **2015**, *4*, e263. [[CrossRef](#)]
108. Xiao, P.; Huang, J.; Dong, T.; Xie, J.; Yuan, J.; Luo, D.; Liu, B. Room-temperature Fabricated Thin-Film Transistors Based on Compounds with Lanthanum and Main Family Element Boron. *Molecules* **2018**, *23*, 1373. [[CrossRef](#)]
109. Liu, B.; Xu, Z.P.; Zou, J.H.; Tao, H.; Xu, M.; Gao, D.Y.; Lan, L.F.; Wang, L.; Ning, H.L.; Peng, J.B. High-performance hybrid white organic light-emitting diodes employing p-type interlayers. *J. Ind. Eng. Chem.* **2015**, *27*, 240–244. [[CrossRef](#)]
110. Liu, B.; Tao, H.; Su, Y.J.; Gao, D.Y.; Lan, L.F.; Zou, J.H.; Peng, J.B. Color-stable, reduced efficiency roll-off hybrid white organic light emitting diodes with ultra high brightness. *Chin. Phys. B* **2013**, *22*, 077303. [[CrossRef](#)]
111. Sun, H.; Chen, Y.H.; Chen, J.S.; Ma, D. Interconnectors in Tandem Organic Light Emitting Diodes and Their Influence on Device Performance. *IEEE J. Sel. Top. Quantum Electron.* **2015**, *22*, 154–163. [[CrossRef](#)]
112. Liao, L.S.; Slusarek, W.K.; Hatwar, T.K.; Ricks, M.L.; Comfort, D.L. Tandem Organic Light-Emitting Diode Using Hexaazatriphenylene Hexacarbonitrile in the Intermediate Connector. *Adv. Mater.* **2008**, *20*, 324–329. [[CrossRef](#)]
113. Tang, J.X.; Fung, M.K.; Lee, C.S.; Lee, S.T. Interface Studies of Intermediate Connectors and Their Roles in Tandem OLEDs. *J. Mater. Chem.* **2010**, *20*, 2539–2548. [[CrossRef](#)]
114. Leem, D.S.; Lee, J.H.; Kim, J.J.; Kang, J.W. Highly Efficient Tandem p-i-n Organic Light-Emitting Diodes Adopting a Low Temperature Evaporated Rhenium Oxide Interconnecting Layer. *Appl. Phys. Lett.* **2008**, *93*, 103304. [[CrossRef](#)]
115. Lai, S.L.; Chan, M.Y.; Fung, M.K.; Lee, C.S. Copper Hexadeca-fluorophthalocyanine and Copper Phthalocyanine as a Pure Organic Connecting Unit in Blue Tandem Organic Light-Emitting Devices. *J. Appl. Phys.* **2007**, *101*, 14509. [[CrossRef](#)]

116. Chen, Y.H.; Chen, J.S.; Ma, D.G.; Yan, D.H.; Wang, L.X.; Chen, Y. Effect of Organic Bulk Heterojunction as Charge Generation Layer on The Performance of Tandem Organic Light-Emitting Diodes. *J. Appl. Phys.* **2011**, *110*, 074504. [[CrossRef](#)]
117. Chen, Y.H.; Chen, J.S.; Ma, D.G.; Yan, D.H.; Wang, L.X.; Zhu, F.R. High Power Efficiency Tandem Organic Light-Emitting Diodes Based on Bulk Heterojunction Organic Bipolar Charge Generatio Layer. *Appl. Phys. Lett.* **2011**, *98*, 243309. [[CrossRef](#)]
118. Liu, J.; Huang, S.; Shi, X.; Wu, X.; Wang, J.; He, G. Charge Separation Process in an Ultrathin Electron-Injecting Bilayer-Assisted Charge Generation Unit for Tandem Organic Light-Emitting Diodes. *J. Phys. Chem. C* **2013**, *117*, 13887–13893. [[CrossRef](#)]
119. Liu, B.; Xu, M.; Wang, L.; Tao, H.; Su, Y.; Gao, D.; Zou, J.; Lan, L.; Peng, J. Comprehensive Study on the Electron Transport Layer in Blue Fluorescent Organic Light-Emitting Diodes. *ECS J. Solid State Sci. Technol.* **2015**, *2*, R258–R261. [[CrossRef](#)]
120. Liu, B.; Xu, M.; Wang, L.; Tao, H.; Su, Y.J.; Gao, D.Y.; Lan, L.F.; Zou, J.H.; Peng, J.B. Simplified hybrid white organic light-emitting diodes with efficiency/efficiency roll-off/color rendering index/color-stability trade-off. *Phys. Status Solidi RRL* **2014**, *8*, 719–723. [[CrossRef](#)]
121. Lee, J.; Chopra, N.; Bera, D.; Maslov, S.; Eom, S.H.; Zheng, Y.; Holloway, P.; Xue, J.; So, F. Down-Conversion White Organic Light-Emitting Diodes Using Microcavity Structure. *Adv. Eng. Mater.* **2011**, *1*, 174–178. [[CrossRef](#)]
122. Du, X.; Tao, S.; Huang, Y.; Yang, X.; Ding, X.; Zhang, X. Efficient Fluorescence/Phosphorescence White Organic Light-Emitting Diodes with Ultra High Color Stability and Mild Efficiency Roll-Off. *Appl. Phys. Lett.* **2015**, *107*, 183304. [[CrossRef](#)]
123. Chen, Y.-H.; Ma, D.-G.; Sun, H.-D.; Chen, J.-S.; Guo, Q.-X.; Wang, Q.; Zhao, Y.-B. Organic Semiconductor Heterojunctions: Electrode-Independent Charge Injectors for High-Performance Organic Light-Emitting Diodes. *Light Sci. Appl.* **2016**, *5*, e16042. [[CrossRef](#)] [[PubMed](#)]
124. Sasabe, H.; Takamatsu, J.; Motoyama, T.; Watanabe, S.; Wagenblast, G.; Langer, N.; Molt, O.; Fuchs, E.; Lennartz, C.; Kido, J. High-Efficiency Blue and White Organic Light-Emitting Devices Incorporating a Blue Iridium Carbene Complex. *Adv. Mater.* **2010**, *22*, 5003–5007. [[CrossRef](#)] [[PubMed](#)]
125. Liu, B.; Lan, L.; Zou, J.; Peng, J. A novel organic light-emitting diode by utilizing double hole injection layer. *Acta Phys. Sin.* **2013**, *62*, 087302.
126. Jiang, C.; Liu, H.; Liu, B.; Zhong, Z.; Zou, J.; Wang, J.; Wang, L.; Peng, J.; Cao, Y. Improved Performance of Inverted Quantum Dots Light Emitting Devices by Introducing Double Hole Transport Layers. *Org. Electron.* **2016**, *31*, 82–89. [[CrossRef](#)]
127. Son, Y.H.; Kim, Y.J.; Park, M.J.; Oh, H.Y.; Park, J.S.; Yang, J.H.; Suh, M.C.; Kwon, J.H. Small single-triplet energy gap bipolar host materials for phosphorescent blue and white organic light emitting diodes. *J. Mater. Chem. C* **2013**, *1*, 5008–5014. [[CrossRef](#)]
128. Zhao, B.; Zhang, T.Y.; Li, W.L.; Su, Z.S.; Chu, B.; Yan, X.W.; Jin, F.M.; Gao, Y.; Wu, H. Organic Electronics Highly efficient and color stable single-emitting-layer fluorescent WOLEDs with delayed fluorescent host. *Org. Electron.* **2015**, *23*, 208–212. [[CrossRef](#)]
129. Liu, B.; Wang, L.; Xu, M.; Tao, H.; Xia, X.; Zou, J.; Su, Y.; Gao, D.; Lan, L.; Peng, J. Simultaneous Achievement of Low Efficiency Roll-Off and Stable Color in Highly Efficient Single-Emitting-Layer Phosphorescent White Organic Light-Emitting Diodes. *J. Mater. Chem. C* **2014**, *2*, 5870–5877. [[CrossRef](#)]
130. Liu, B.; Wang, L.; Zou, J.H.; Tao, H.; Su, Y.J.; Gao, D.Y.; Xu, M.; Lan, L.F.; Peng, J.B. Investigation on spacers and structures: A simple but effective approach toward high-performance hybrid white organic light emitting diodes. *Synth. Met.* **2013**, *184*, 5–9. [[CrossRef](#)]
131. Yin, Y.M.; Yu, J.; Cao, H.T.; Zhang, L.T.; Sun, H.Z.; Xie, W.F. Efficient non-doped phosphorescent orange, blue and white organic light-emitting devices. *Sci. Rep.* **2014**, *4*, 6754. [[CrossRef](#)] [[PubMed](#)]
132. Wang, L.; Liu, B.; Zhao, X.; Demir, H.V.; Gu, H.; Sun, H. Solvent-Assisted Surface Engineering for High Performance All-Inorganic Perovskite Nanocrystals Light-Emitting Diodes. *ACS Appl. Mater. Interfaces* **2018**, *10*, 19828–19835. [[CrossRef](#)] [[PubMed](#)]
133. Liu, B.; Xu, M.; Wang, L.; Zou, J.H.; Tao, H.; Su, Y.J.; Gao, D.Y.; Ning, H.L.; Lan, L.F.; Peng, J.B. Regulating charges and excitons in simplified hybrid white organic light-emitting diodes: The key role of concentration in single dopant host-guest systems. *Org. Electron.* **2014**, *15*, 2616–2623. [[CrossRef](#)]

134. Liu, B.; Zou, J.H.; Su, Y.J.; Gao, D.Y.; Lan, L.F.; Tao, H.; Peng, J.B. Hybrid white organic light emitting diodes with low efficiency roll-off, stable color and extreme brightness. *J. Lumin.* **2014**, *151*, 161–164. [[CrossRef](#)]
135. Chen, B.; Liu, B.; Zeng, J.; Nie, H.; Xiong, Y.; Zou, J.; Ning, H.; Wang, Z.; Zhao, Z.; Tang, B.Z. Efficient Bipolar Blue AIEgens for High-Performance Nondoped Blue OLEDs and Hybrid White OLEDs. *Adv. Func. Mater.* **2018**, *28*, 1803369. [[CrossRef](#)]
136. Zhang, M.; Chen, Z.; Xiao, L.; Qu, B.; Gong, Q. High-Color-Quality White Top-Emitting Organic Electroluminescent Devices Based on Both Exciton and Electroplex Emission. *Appl. Phys. Express* **2013**, *4*, 784–788. [[CrossRef](#)]
137. Luo, D.X.; Xiao, Y.; Hao, M.M.; Zhao, Y.; Yang, Y.B.; Gao, Y.; Liu, B. Doping-free white organic light-emitting diodes without blue molecular emitter: An unexplored approach to achieve high performance via exciplex emission. *Appl. Phys. Lett.* **2017**, *110*, 061105. [[CrossRef](#)]
138. Schwartz, G.; Pfeiffer, M.; Reineke, S.; Walzer, K.; Leo, K. Harvesting Triplet Excitons from Fluorescent Blue Emitters in White Organic Light-Emitting Diodes. *Adv. Mater.* **2007**, *19*, 3672–3676. [[CrossRef](#)]
139. Ye, J.; Zheng, C.-J.; Ou, X.-M.; Zhang, X.-H.; Fung, M.-K.; Lee, C.-S. Management of Singlet and Triplet Excitons in a Single Emission Layer: A Simple Approach for a High-Efficiency Fluorescence/Phosphorescence Hybrid White Organic Light-Emitting Device. *Adv. Mater.* **2012**, *24*, 3410–3414. [[CrossRef](#)]
140. Liu, B.; Delikanli, S.; Gao, Y.; Gungor, K.; Demir, H.V. Nanocrystal light-emitting diodes based on type II nanoplatelets. *Nano Energy* **2018**, *47*, 115–122. [[CrossRef](#)]
141. Chapran, M.; Angioni, E.; Findlay, N.J.; Breig, B.; Cherpak, V.; Stakhira, P.; Tuttle, T.; Volyniuk, D.; Grazulevicius, J.V.; Nastishin, Y.A.; et al. An ambipolar BODIPY derivative for a white exciplex OLED and cholesteric liquid crystal laser towards multi-functional devices. *ACS Appl. Mater. Interfaces* **2017**, *9*, 4750–4757. [[CrossRef](#)] [[PubMed](#)]
142. Cekaviciute, M.; Simokaitiene, J.; Volyniuk, D.; Sini, G.; Grazulevicius, J.V. Arylfluorenyl-substituted methoxytriphenylamines as deep blue exciplex forming bipolar semiconductors for white and blue organic light emitting diodes. *Dyes Pigments* **2017**, *140*, 187–202. [[CrossRef](#)]
143. Yokoyama, M.; Su, S.H.; Hou, C.C.; Wu, C.T.; Kung, C.H. Highly Efficient White Organic Light-Emitting Diodes with a p-i-n Tandem Structure. *Jpn. J. Appl. Phys.* **2011**, *50*, 04DK06. [[CrossRef](#)]
144. Hoa, M.H.; Chen, T.M. Highly Efficient p-i-n White Organic Light Emitting Devices with Tandem Structure. *Appl. Phys. Lett.* **2007**, *91*, 233507. [[CrossRef](#)]
145. Berggren, M.; Gustafsson, G.; Inganäs, O.; Andersson, M.R.; Hjertberg, T.; Wennerström, O. White Light from an Electroluminescent Diode Made from Poly[3(4-Octylphenyl)-2,2'-Bithiophene] and an Oxadiazole Derivative. *J. Appl. Phys.* **1994**, *76*, 7530–7534. [[CrossRef](#)]
146. Feng, J.; Li, F.; Gao, W.; Liu, S.; Wang, Y. White Light Emission from Exciplex Using Tris-(8-Hydroxyquinoline)Aluminum as Chromaticity-Tuning Layer. *Appl. Phys. Lett.* **2001**, *78*, 3947–3949. [[CrossRef](#)]
147. Gebler, D.D.; Wang, Y.Z.; Blatchford, J.W.; Jessen, S.W. Exciplex Emission in Bilayer Polymer Light-Emitting Devices. *Appl. Phys. Lett.* **1997**, *70*, 1644–1646. [[CrossRef](#)]
148. Chen, S.; Zhao, X.; Wu, Q.; Shi, H.; Mei, Y.; Zhang, R.; Wang, L.; Huang, W. Efficient, Color-Stable Flexible White Top-Emitting Organic Light-Emitting Diodes. *Org. Electron.* **2013**, *14*, 3037–3045. [[CrossRef](#)]
149. Yook, K.S.; Jeon, S.O.; Joo, C.W.; Lee, J.Y. Color stability and suppressed efficiency roll-off in white organic light-emitting diodes through management of interlayer and host properties. *J. Ind. Eng. Chem.* **2009**, *15*, 420–422. [[CrossRef](#)]
150. Su, S.-J.; Gonmori, E.; Sasabe, H.; Kido, J. Highly efficient organic blue- and white-light-emitting devices having a carrier- and exciton-confining structure for reduced efficiency roll-off. *Adv. Mater.* **2008**, *20*, 4189–4194. [[CrossRef](#)]
151. Reineke, S.; Lindner, F.; Schwartz, G.; Seidler, N.; Walzer, K.; Lüssem, B.; Leo, K. White organic light-emitting diodes with fluorescent tube efficiency. *Nature* **2009**, *459*, 234–238. [[CrossRef](#)] [[PubMed](#)]
152. Zhu, L.; Wu, Z.; Chen, J.; Ma, D. Reduced Efficiency Roll-Off in All-Phosphorescent White Organic Light-Emitting Diodes with an External Quantum Efficiency of Over 20%. *J. Mater. Chem. C* **2015**, *3*, 3304–3310. [[CrossRef](#)]
153. Fleetham, T.; Ecton, J.; Wang, Z.; Bakken, N. Single-Doped White Organic Light-Emitting Device with an External Quantum Efficiency Over 20%. *Adv. Mater.* **2013**, *25*, 2573–2576. [[CrossRef](#)] [[PubMed](#)]

154. Xu, L.; Tang, C.W.; Rothberg, L.J. High Efficiency Phosphorescent White Organic Light-Emitting Diodes with An Ultra-Thin Red and Green Co-Doped Layer and Dual Blue Emitting Layers. *Org. Electron.* **2016**, *32*, 54–58. [[CrossRef](#)]
155. Kanno, H.; Holmes, R.J.; Sun, Y.; Kena, S.; Forrest, S.R. White Stacked Electrophosphorescent Organic Light-Emitting Devices Employing MoO₃ as a Charge-Generation Layer. *Adv. Mater.* **2006**, *18*, 339–342. [[CrossRef](#)]
156. Wu, H.; Zou, J.; Liu, F.; Wang, L.; Mikhailovsky, A.; Bazan, G.C.; Yang, W.; Cao, Y. Efficient Single Active Layer Electrophosphorescent White Polymer Light-Emitting Diodes. *Adv. Mater.* **2008**, *20*, 696. [[CrossRef](#)]
157. Wei, P.C.; Zhang, D.D.; Cai, M.H.; Song, X.Z.; Wang, Z.Y.; Duan, L. Simplified Single-Emitting-Layer Hybrid White Organic Light-Emitting Diodes with High Efficiency, Low Efficiency Roll-Off, High Color Rendering Index and Superior Color. *Org. Electron.* **2017**, *49*, 242–248. [[CrossRef](#)]
158. Pereira, D.; Pinto, A.; Califórnia, A.; Gomes, J. Control of A White Organic Light Emitting Diode Emission Parameters Using A Single Doped RGB Active Layer. *Mater. Sci. Eng. B* **2016**, *211*, 156–165. [[CrossRef](#)]
159. Sun, N.; Wang, Q.; Zhao, Y.B.; Chen, Y.H.; Yang, D.Z.; Zhao, F.C.; Chen, J.S.; Ma, D.G. High-Performance Hybrid White Organic Light-Emitting Devices without Interlayer between Fluorescent and Phosphorescent Emissive Regions. *Adv. Mater.* **2014**, *26*, 1617–1621. [[CrossRef](#)]
160. Ban, X.; Sun, K.; Sun, Y.; Huang, B.; Jiang, W. Design of High Triplet Energy Electron Transporting Material for Exciplex-Type Host: Efficient Blue and White Phosphorescent OLEDs based on Solution Processing. *Org. Electron.* **2016**, *33*, 9–14. [[CrossRef](#)]
161. Wang, Q.; Ding, J.; Ma, D.; Cheng, Y.; Wang, L.; Jing, X.; Wang, F. Harvesting Excitons Via Two Parallel Channels for Efficient White Organic LEDs with Nearly 100% Internal Quantum Efficiency: Fabrication and Emission Mechanism Analysis. *Adv. Funct. Mater.* **2009**, *19*, 84–95. [[CrossRef](#)]
162. Wang, Q.; Ding, J.Q.; Zhang, Z.Q.; Ma, D.G.; Cheng, Y.X.; Wang, L.X.; Wang, F.S. A high-performance tandem white organic light-emitting diode combining highly effective white-units and their interconnection layer. *J. Appl. Phys.* **2009**, *105*, 076101. [[CrossRef](#)]
163. Lee, S.; Shin, H.; Kim, J.J. High-Efficiency Orange and Tandem White Organic Light-Emitting Diodes Using Phosphorescent Dyes with Horizontally Oriented Emitting Dipoles. *Adv. Mater.* **2014**, *26*, 5864–5868. [[CrossRef](#)] [[PubMed](#)]
164. Lee, S.; Kim, K.H.; Limbach, D.; Park, Y.S.; Kim, J.J. Organic Light Emitting Diodes: Low Roll-Off and High Efficiency Orange Organic Light Emitting Diodes with Controlled Co-Doping of Green and Red Phosphorescent Dopants in an Exciplex Forming Co-Host. *Adv. Funct. Mater.* **2013**, *23*, 4061–4062. [[CrossRef](#)]
165. Lee, S.; Limbach, D.; Kim, K.H.; Yoo, S.J.; Park, Y.S.; Kim, J.J. High Efficiency and Non-Color-Changing Orange Organic Light Emitting Diodes with Red and Green Emitting Layers. *Org. Electron.* **2013**, *14*, 1856–1860. [[CrossRef](#)]
166. Park, Y.S.; Lee, S.; Kim, K.H.; Kim, S.Y.; Lee, J.H.; Kim, J.J. Exciplex-Forming Co-host for Organic Light-Emitting Diodes with Ultimate Efficiency. *Adv. Funct. Mater.* **2013**, *23*, 4914–4920. [[CrossRef](#)]
167. Chao, C.I.; Chen, S.A. White Light Emission from Exciplex in a Bilayer Device with Two Blue Light-Emitting Polymers. *Appl. Phys. Lett.* **1998**, *73*, 426–428. [[CrossRef](#)]
168. Cherpak, V.; Stakhira, P.; Minaev, B.; Baryshnikov, G.; Stromylo, E.; Helzhynskyy, I.; Chapran, M.; Volyniuk, D.; Hotra, Z.; Dabulienė, A.; et al. Mixing of Phosphorescent and Exciplex Emission in Efficient Organic Electroluminescent Devices. *ACS Appl. Mater. Interfaces* **2015**, *7*, 1219–1225. [[CrossRef](#)]
169. Zhao, Y.B.; Chen, J.S.; Ma, D.G. Ultrathin Nondoped Emissive Layers for Efficient and Simple Monochrome and White Organic Light-Emitting Diodes. *ACS Appl. Mater. Interfaces* **2013**, *5*, 965–971. [[CrossRef](#)]
170. Xue, K.W.; Han, G.G.; Duan, Y.; Chen, P.; Yang, Y.Q.; Yang, D.; Duan, Y.H.; Wang, X.; Zhao, Y. Doping-free orange and white phosphorescent organic light-emitting diodes with ultra-simple structure and excellent color stability. *Org. Electron.* **2015**, *18*, 84–88. [[CrossRef](#)]
171. Xue, K.W.; Sheng, R.; Duan, Y.; Chen, P.; Chen, B.Y.; Wang, X.; Duan, Y.H.; Zhao, Y. Efficient non-doped monochrome and white phosphorescent organic light-emitting diodes based on ultrathin emissive layers. *Org. Electron.* **2015**, *26*, 451–457. [[CrossRef](#)]
172. Fleetham, T.; Li, G.; Li, J. Phosphorescent Pt (II) and Pd (II) Complexes for Efficient, High-Color-Quality, and Stable OLEDs. *Adv. Mater.* **2017**, *29*, 1601861. [[CrossRef](#)] [[PubMed](#)]
173. Fleetham, T.; Li, G.; Wen, L.; Li, J. Efficient “Pure” Blue OLEDs Employing Tetradentate Pt Complexes with a Narrow Spectral Bandwidth. *Adv. Mater.* **2014**, *26*, 7116–7121. [[CrossRef](#)] [[PubMed](#)]

174. Coburn, C.; Jeong, C.; Forrest, S.R. Reliable, All-Phosphorescent Stacked White Organic Light Emitting Devices with a High Color Rendering Index. *ACS Photon.* **2018**, *5*, 630–635. [[CrossRef](#)]
175. Rajamalli, P.; Senthilkumar, N.; Gandeepan, P.; Huang, P.-Y.; Huang, M.-J.; Yang, C.-Y.; Chiu, M.-J.; Chu, L.-K.; Lin, H.-W.; Cheng, C.-H. A New Molecular Design Based on Thermally Activated Delayed Fluorescence for Highly Efficient Organic Light Emitting Diodes. *J. Am. Chem. Soc.* **2016**, *138*, 628–634. [[CrossRef](#)] [[PubMed](#)]
176. Yang, Z.Y.; Mao, Z.; Xie, Z.L.; Zhang, Y.; Liu, S.W.; Zhao, J.; Xu, J.R.; Chi, Z.G.; Aldred, M.P. Recent advances in organic thermally activated delayed fluorescence materials. *Chem. Soc. Rev.* **2017**, *46*, 915–1016. [[CrossRef](#)] [[PubMed](#)]
177. Zhang, D.D.; Cai, M.H.; Zhang, Y.G.; Zhang, D.Q.; Duan, L. Sterically Shielded Blue Thermally Activated Delayed Fluorescence Emitters with Improved Efficiency and Stability. *Mater. Horiz.* **2016**, *3*, 145–151. [[CrossRef](#)]
178. Tao, Y.; Yuan, K.; Chen, T.; Xu, P.; Li, H.; Chen, R.; Zheng, C.; Zhang, L.; Huang, W. Thermally Activated Delayed Fluorescence Materials Towards the Breakthrough of Organoelectronics. *Adv. Mater.* **2014**, *26*, 7931–7958. [[CrossRef](#)]
179. Masui, K.; Nakanotani, H.; Adachi, C. Analysis of exciton annihilation in high efficiency sky-blue organic light-emitting diodes with thermally activated delayed fluorescence. *Org. Electron.* **2013**, *14*, 2721–2726. [[CrossRef](#)]
180. Zhang, D.; Duan, L.; Li, C.; Li, Y.; Li, H.; Zhang, D.; Qiu, Y. High-Efficiency Fluorescent Organic Light-Emitting Devices Using Sensitizing Hosts with a Small Singlet-Triplet Exchange Energy. *Adv. Mater.* **2014**, *26*, 5050–5055. [[CrossRef](#)]
181. Guo, J.J.; Li, X.L.; Nie, H.; Luo, W.W.; Gan, S.F.; Hu, S.M.; Hu, R.R.; Qin, A.J.; Zhao, Z.J.; Su, S.J.; et al. Achieving High-Performance Nondoped OLEDs with Extremely Small Efficiency Roll-Off by Combining Aggregation-Induced Emission and Thermally Activated Delayed Fluorescence. *Adv. Funct. Mater.* **2017**, *27*, 1606458. [[CrossRef](#)]
182. Yong, J.C.; Yook, K.S.; Lee, J.Y. Cool and Warm Hybrid White Organic Light-Emitting Diode with Blue Delayed Fluorescent Emitter Both as Blue Emitter and Triplet Host. *Sci. Rep.* **2015**, *5*, 7859.
183. Wu, Z.; Qi, W.; Ling, Y.; Chen, J.; Qiao, X.; Ahamad, T.; Alshehri, S.M.; Yang, C.; Ma, D. Managing excitons and charges for high-performance fluorescent white organic light-emitting diodes. *ACS Appl. Mater. Interfaces* **2016**, *8*, 28780–28788. [[CrossRef](#)] [[PubMed](#)]
184. Hou, L.; Duan, L.; Qiao, J.; Zhang, D.; Dong, G.; Wang, L.; Qiu, Y. Efficient Solution-Processed Small-Molecule Single Emitting Layer Electrophosphorescent White Light-Emitting Diodes. *Org. Electron.* **2010**, *11*, 1344–1350. [[CrossRef](#)]
185. Wang, Q.; Oswald, I.W.H.; Perez, M.R.; Jia, H.P.; Shahub, A.A.; Qiao, Q.Q.; Gnade, B.E.; Omary, M.A. Doping-Free Organic Light-Emitting Diodes with Very High Power Efficiency, Simple Device Structure, and Superior Spectral Performance. *Adv. Funct. Mater.* **2014**, *24*, 4746–4752. [[CrossRef](#)]
186. Wang, J.; Chen, J.; Qiao, X.; Alshehri, S.M.; Ahamad, T.; Ma, F. Simple-Structured Phosphorescent Warm White Organic Light-Emitting Diodes with High Power Efficiency and Low Efficiency Roll-off. *ACS Appl. Mater. Interfaces* **2016**, *8*, 10093–10097. [[CrossRef](#)] [[PubMed](#)]
187. Nishide, J.-I.; Nakanotani, H.; Hiraga, Y.; Adachi, C. High-efficiency white organic light-emitting diodes using thermally activated delayed fluorescence. *Appl. Phys. Lett.* **2014**, *104*, 233304. [[CrossRef](#)]
188. Wu, Z.; Luo, J.J.; Sun, N.; Zhu, L.P.; Sun, H.D.; Yu, L.; Yang, D.Z.; Qiao, X.F.; Chen, J.S.; Yang, C.L.; et al. HighPerformance Hybrid White Organic Light-Emitting Diodes with Superior Efficiency/Color Rendering Index/Color Stability and Low Efficiency Roll-Off Based on a Blue Thermally Activated Delayed Fluorescent Emitter. *Adv. Funct. Mater.* **2016**, *26*, 3306–3313. [[CrossRef](#)]
189. Luo, D.; Chen, Q.; Gao, Y.; Zhang, M.; Liu, B. Extremely Simplified, High-Performance and Doping-Free White Organic Light-Emitting Diodes Based on Single Thermally Activated Delayed Fluorescent Emitter. *ACS Energy Lett.* **2018**, *3*, 1531–1538. [[CrossRef](#)]
190. Kim, B.S.; Yook, K.S.; Lee, J.Y. Above 20% External Quantum Efficiency in Novel Hybrid White Organic Light-Emitting Diodes Having Green Thermally Activated Delayed Fluorescent Emitter. *Sci. Rep.* **2014**, *4*, 6019. [[CrossRef](#)]
191. Goushi, K.; Yoshida, K.; Sato, K.; Adachi, C. Organic light-emitting diodes employing efficient reverse intersystem crossing for triplet-to-singlet state conversion. *Nat. Photon.* **2012**, *6*, 253–258. [[CrossRef](#)]

192. Goushi, K.; Adachi, C. Efficient Organic Light-Emitting Diodes through Up-Conversion from Triplet to Singlet Excited States of Exciplexes. *Appl. Phys. Lett.* **2012**, *101*, 3174–3187. [[CrossRef](#)]
193. Chen, D.; Liu, K.; Gan, L.; Liu, M.; Gao, K.; Xie, G.; Ma, Y.; Cao, Y.; Su, S.-J. Modulation of Exciton Generation in Organic Active Planar pn Heterojunction: Toward Low Driving Voltage and High-Efficiency OLEDs Employing Conventional and Thermally Activated Delayed Fluorescent Emitters. *Adv. Mater.* **2016**, *28*, 6758–6765. [[CrossRef](#)] [[PubMed](#)]
194. Liu, X.; Chen, Z.; Zheng, C.; Liu, C.; Lee, C.; Li, F.; Ou, X.-M.; Zhang, X.-H. Prediction and Design of Efficient Exciplex Emitters for High-Efficiency, Thermally Activated Delayed-Fluorescence Organic Light-Emitting Diodes. *Adv. Mater.* **2015**, *27*, 2378–2383. [[CrossRef](#)] [[PubMed](#)]
195. Liu, X.; Chen, Z.; Zheng, C.-J.; Chen, M.; Liu, W.; Zhang, X.-H.; Lee, C.-S. Nearly 100% Triplet Harvesting in Conventional Fluorescent Dopant-Based Organic Light-Emitting Devices through Energy Transfer from Exciplex. *Adv. Mater.* **2015**, *27*, 2025–2030. [[CrossRef](#)] [[PubMed](#)]
196. Zhang, T.; Chu, B.; Li, W.; Su, Z.; Peng, Q.M.; Zhao, B.; Luo, Y.; Jin, F.; Yan, X.; Gao, Y.; et al. Efficient Triplet Application in Exciplex Delayed-Fluorescence OLEDs Using a Reverse Intersystem Crossing Mechanism Based on a ΔE_S -T of Around Zero. *ACS Appl. Mater. Interfaces* **2014**, *6*, 11907. [[CrossRef](#)] [[PubMed](#)]
197. Hung, W.Y.; Fang, G.C.; Lin, S.W.; Cheng, S.H.; Wong, K.T.; Kuo, T.Y.; Chou, P.T. The First Tandem, All-exciplex-based WOLED. *Sci. Rep.* **2014**, *4*, 5161. [[CrossRef](#)]
198. Zhao, B.; Zhang, T.; Chu, B.; Li, W.; Su, Z.; Luo, Y.; Li, R.; Yan, X.; Jin, F.; Gao, Y.; et al. Highly efficient tandem full exciplex orange and warm white OLEDs based on thermally activated delayed fluorescence mechanism. *Org. Electron.* **2015**, *17*, 15–21. [[CrossRef](#)]
199. Li, F.; Cheng, G.; Zhao, Y.; Feng, J.; Liu, S.Y.; Zhang, M.; Ma, Y.G.; Shen, J.C. White-electrophosphorescence devices based on rhenium complexes. *Appl. Phys. Lett.* **2003**, *83*, 4716. [[CrossRef](#)]
200. Sun, Y.R.; Giebink, N.C.; Kanno, H.; Ma, B.W.; Thompson, M.E.; Forrest, S.R. Management of Singlet and Triplet Excitons for Efficient White Organic Light-Emitting Devices. *Nature* **2006**, *440*, 908–912. [[CrossRef](#)]
201. Chen, Z.; Liu, X.K.; Zheng, C.J.; Ye, J.; Liu, C.L.; Li, F.; Ou, X.M.; Lee, C.S.; Zhang, X.H. High Performance Exciplex-Based Fluorescence-Phosphorescence White Organic Light-Emitting Device with Highly Simplified Structure. *Chem. Mater.* **2015**, *27*, 5206–5211. [[CrossRef](#)]
202. Li, X.L.; Ouyang, X.H.; Chen, D.C.; Cai, X.Y.; Liu, M.; Ge, Z.Y.; Cao, Y.; Su, S.J. Highly efficient blue and warm white organic light-emitting diodes with a simplified structure. *Nanotechnology* **2016**, *27*, 124001. [[CrossRef](#)] [[PubMed](#)]
203. Liu, B.; Wang, L.; Gao, D.Y.; Zou, J.H.; Ning, H.L.; Peng, J.B.; Cao, Y. Extremely high-efficiency and ultrasimplified hybrid white organic light-emitting diodes exploiting double multifunctional blue emitting layers. *Light Sci. Appl.* **2016**, *5*, e16137. [[CrossRef](#)] [[PubMed](#)]
204. Zheng, C.-J.; Wang, J.; Ye, J.; Lo, M.-F.; Liu, X.-K.; Fung, M.-K.; Zhang, X.-H.; Lee, C.-S. Novel Efficient Blue Fluorophors with Small Singlet-Triplet Splitting: Hosts for Highly Efficient Fluorescence and Phosphorescence Hybrid WOLEDs with Simplified Structure. *Adv. Mater.* **2013**, *25*, 2205–2211. [[CrossRef](#)] [[PubMed](#)]
205. Schwartz, G.; Reineke, S.; Walzer, K.; Leo, K. Reduced efficiency roll-off in high-efficiency hybrid white organic light-emitting diodes. *Appl. Phys. Lett.* **2008**, *92*, 053311. [[CrossRef](#)]
206. Kanno, H.; Giebink, N.C.; Sun, Y.; Forrest, S.R. Stacked white organic light-emitting devices based on a combination of fluorescent and phosphorescent emitters. *Appl. Phys. Lett.* **2006**, *89*, 023503. [[CrossRef](#)]
207. Schwartz, G.; Ke, T.-H.; Wu, C.-C.; Walzer, K.; Leo, K. Balanced ambipolar charge carrier mobility in mixed layers for application in hybrid white organic light-emitting diodes. *Appl. Phys. Lett.* **2008**, *93*, 073304. [[CrossRef](#)]
208. Zhang, T.; Zhao, B.; Chu, B.; Li, W.; Su, Z.; Yan, X.; Liu, C.; Wu, H.; Gao, Y.; Jin, F.; et al. Simple structured hybrid WOLEDs based on incomplete energy transfer mechanism: From blue exciplex to orange dopant. *Sci. Rep.* **2015**, *5*, 10234. [[CrossRef](#)]
209. Luo, D.; Li, X.-L.; Zhao, Y.; Gao, Y.; Liu, B. High-Performance Blue Molecular Emitter-Free and Doping-Free Hybrid White Organic Light-Emitting Diodes: An Alternative Concept to Manipulate Charges and Excitons Based on Exciplex and Electroplex Emission. *ACS Photon.* **2017**, *4*, 1566–1575. [[CrossRef](#)]
210. Rosenow, T.C.; Furno, M.; Reineke, S.; Olthof, S.; Lussem, B.; Leo, K. Highly efficient white organic light-emitting diodes based on fluorescent blue emitters. *J. Appl. Phys.* **2010**, *108*, 113113. [[CrossRef](#)]

211. Schwab, T.; Schubert, S.; Hofmann, S.; Frobel, M.; Fuchs, C.; Thomschke, M.; Muller-Meskamp, L.; Leo, K.; Gather, M.C. Highly Efficient and Color Stable Inverted White Top-emitting OLEDs with Ultra-thin Wetting Layer Top Electrodes. *Adv. Opt. Mater.* **2013**, *1*, 707–713. [[CrossRef](#)]
212. Gaynor, W.; Hofmann, S.; Christoforo, M.G.; Sachse, C.; Mehra, S.; Salleo, A.; McGehee, M.D.; Gather, M.C.; Lussem, B.; Muller-Meskamp, L. Color in the Corners: ITO-Free White OLEDs with Angular Color Stability. *Adv. Mater.* **2013**, *25*, 4006–4013. [[CrossRef](#)] [[PubMed](#)]
213. Thomschke, M.; Reineke, S.; Lussem, B.; Leo, K. Highly efficient white top-emitting organic light-emitting diodes comprising laminated microlens films. *Nano Lett.* **2012**, *12*, 424–428. [[CrossRef](#)] [[PubMed](#)]
214. Zhang, M.; Wang, K.; Zheng, C.-J.; Liu, W.; Lin, H.; Tao, S.-L.; Zhang, X.-H. Efficient, color-stable and high color-rendering-index white organic light-emitting diodes employing full thermally activated delayed fluorescence system. *Org. Electron.* **2017**, *50*, 466–472. [[CrossRef](#)]
215. Duan, L.; Tsuboi, T.; Qiu, Y.; Li, Y.R.; Zhang, G.H. Tandem organic light-emitting diodes with KBH4 doped 9,10-bis(3-(pyridin-3-yl)phenyl) anthracene connected to the charge generation layer. *Opt. Express* **2012**, *20*, 14564. [[CrossRef](#)] [[PubMed](#)]
216. Huang, C.; Xie, Y.; Wu, S.; Li, S.H.; Liang, J.J.; Fung, M.K. Thermally activated delayed fluorescence-based tandem OLEDs with very high external quantum efficiency. *Phys. Status Solidi A* **2017**, *214*, 1700240. [[CrossRef](#)]
217. Chen, S.; Qu, Q.; Kong, M.; Zhao, X.; Yu, Z.; Jia, P.; Huang, W. On the Origin of the Shift in Color in White Organic Light-Emitting Diodes. *J. Mater. Chem. C* **2013**, *1*, 3508. [[CrossRef](#)]
218. Zhao, B.; Zhang, H.; Miao, Y.; Wang, Z.; Gao, L.; Wang, H.; Hao, Y.; Li, W. High Color Stability and CRI (>80) Fluorescent White Organic Light-Emitting Diode based Pure Emission of Exciplexes by Employing Merely Complementary colors. *J. Mater. Chem. C* **2018**, *6*, 304–311. [[CrossRef](#)]
219. Fröbel, M.; Schwab, T.; Kliem, M.; Hofmann, S.; Leo, K.; Gather, M.C. Get It White: Color-Tunable Ac/Dc OLEDs. *Light Sci. Appl.* **2015**, *4*, e247. [[CrossRef](#)]
220. Wang, D.; Li, W.L.; Su, Z.S.; Li, T.L.; Chu, B.; Bi, D.F.; Chen, L.L.; Su, W.M.; He, H. Broad Wavelength Modulating and Design of Organic White Diode Based on Lighting by Using Exciplex Emission from Mixed Acceptors. *Appl. Phys. Lett.* **2006**, *89*, 53. [[CrossRef](#)]
221. Gong, S.; Chen, Y.; Luo, J.; Yang, C.; Zhong, C.; Qin, J.; Ma, D. Bipolar Tetraarylsilanes as Universal Hosts for Blue, Green, Orange, and White Electrophosphorescence with High Efficiency and Low Efficiency Roll-Off. *Adv. Funct. Mater.* **2011**, *21*, 1168–1178. [[CrossRef](#)]
222. Liu, B.; Tao, H.; Wang, L.; Gao, D.Y.; Liu, W.C.; Zou, J.H.; Xu, M.; Ning, H.L.; Peng, J.B.; Cao, Y. High-performance doping-free hybrid white organic light-emitting diodes: The exploitation of ultrathin emitting nanolayers (<1 nm). *Nano Energy* **2016**, *26*, 26–36.
223. Luo, D.; Xiao, P.; Liu, B. Doping-Free White Organic Light-Emitting Diodes. *Chem. Rec.* **2018**. [[CrossRef](#)]
224. Liu, B.; Wang, L.; Tao, H.; Xu, M.; Zou, J.; Ning, H.; Peng, J.; Cao, Y. Doping-Free Tandem White Organic Light-Emitting Diodes. *Sci. Bull.* **2017**, *62*, 1193–1200. [[CrossRef](#)]
225. Yoshihiro, O. Color rendering and luminous efficacy of white LED spectra. *Proc. SPIE* **2004**, *88*, 5530.
226. Adachi, C.; Baldo, M.A.; Thompson, M.E.; Forrest, S.R. Nearly 100% Internal Phosphorescence Efficiency in an Organic Light-Emitting Device. *J. Appl. Phys.* **2001**, *90*, 5048–5051. [[CrossRef](#)]
227. Nozoe, S.; Matsuda, M. Enhanced emission by accumulated charges at organic/metal interfaces generated during the reverse bias of organic light emitting diodes. *Appl. Sci.* **2017**, *7*, 1045. [[CrossRef](#)]
228. Brovelli, S.; Sforazzini, G.; Serri, M.; Winroth, G.; Suzuk, K.; Meinardi, F.; Anderson, H.L.; Cacialli, F. Emission Color Trajectory and White Electroluminescence Through Supramolecular Control of Energy Transfer and Exciplex Formation in Binary Blends of Conjugated Polyrotaxanes. *Adv. Funct. Mater.* **2012**, *22*, 4284–4291. [[CrossRef](#)]
229. Preinfalk, J.B.; Eiselt, T.; Wehlius, T.; Rohnacher, V.; Hanemann, T.; Gomard, G.; Lemmer, U. Large-Area Screen-Printed Internal Extraction Layers for Organic Light-Emitting Diodes. *ACS Photon.* **2017**, *4*, 928–933. [[CrossRef](#)]
230. Koh, T.-W.; Spechler, J.A.; Lee, K.M.; Arnold, C.B.; Rand, B.P. Enhanced Outcoupling in Organic Light-Emitting Diodes via a High-Index Contrast Scattering Layer. *ACS Photon.* **2015**, *2*, 1366–1372. [[CrossRef](#)]
231. Krotkus, S.; Kasemann, D.; Lenk, S.; Leo, K.; Reineke, S. Adjustable White-Light Emission from a Photo-Structured Micro-OLED Array. *Light Sci. Appl.* **2016**, *5*, e16121. [[CrossRef](#)] [[PubMed](#)]

232. Ji, W.; Zhang, L.; Gao, R.; Zhang, L.; Xie, W.; Zhang, H.; Li, B. Top-Emitting White Organic Light-Emitting Devices with Down-Conversion Phosphors: Theory and Experiment. *Opt. Express* **2008**, *16*, 15489. [[CrossRef](#)] [[PubMed](#)]
233. Jiang, C.; Zhong, Z.; Liu, B.; He, Z.; Zou, J.; Wang, L.; Wang, J.; Peng, J.B.; Cao, Y. Coffee-Ring-Free Quantum Dot Thin Film Using Inkjet Printing from a Mixed-Solvent System on Modified ZnO Transport Layer for Light-Emitting Devices. *ACS Appl. Mater. Interfaces* **2016**, *8*, 26162–26168. [[CrossRef](#)] [[PubMed](#)]
234. Liu, B.; Wang, L.; Gu, H.; Sun, H.; Demir, H.V. Highly Efficient Green Light-Emitting Diodes from All-Inorganic Perovskite Nanocrystals Enabled by a New Electron Transport Layer. *Adv. Opt. Mater.* **2018**, *5*, 1800220. [[CrossRef](#)]
235. Xiao, P.; Huang, J.; Yan, D.; Luo, D.; Yuan, J.; Liu, B.; Liang, D. Emergence of Nanoplatelet Light-Emitting Diodes. *Materials* **2018**, *11*, 1376. [[CrossRef](#)] [[PubMed](#)]
236. Gao, Y.; Li, M.; Delikanli, S.; Zheng, H.; Liu, B.; Dang, C.; Sum, T.C.; Demir, H.V. Low-threshold lasing from colloidal CdSe/CdSeTe core/alloyed-crown type-II heteronanoplatelets. *Nanoscale* **2018**, *10*, 9466–9475. [[CrossRef](#)] [[PubMed](#)]
237. Shi, Z.; Li, Y.; Zhang, Y.; Chen, Y.; Li, X.; Wu, D.; Xu, T.; Shan, C.; Du, G. High-efficiency and air-stable perovskite quantum dots light-emitting diodes with an all-inorganic heterostructure. *Nano Lett.* **2016**, *17*, 313–321. [[CrossRef](#)] [[PubMed](#)]
238. Shi, Z.; Li, S.; Li, Y.; Ji, H.; Li, X.; Wu, D.; Xu, T.; Chen, Y.; Tian, Y.; Zhang, Y.; et al. Strategy of solution-processed all-inorganic heterostructure for humidity/temperature-stable perovskite quantum dot light-emitting diodes. *ACS Nano* **2018**, *12*, 1462–1472. [[CrossRef](#)] [[PubMed](#)]



© 2019 by the authors. Licensee MDPI, Basel, Switzerland. This article is an open access article distributed under the terms and conditions of the Creative Commons Attribution (CC BY) license (<http://creativecommons.org/licenses/by/4.0/>).